AIMS Mathematics, 9(3): 6803–6831.
DOI: 10.3934/math.2024332
Received: 13 September 2023
Revised: 11 January 2024
Accepted: 29 January 2024
Published: 19 February 2024

http://www.aimspress.com/journal/Math

Research article

Finite-time adaptive prescribed performance DSC for pure feedback nonlinear systems with input quantization and unmodeled dynamics

Bin Hang[1] **and Weiwei Deng**[2,*]

[1] School of Automation, Northwestern Polytechnical University, Xi'an 710072, China
[2] College of Information Engineering, Yangzhou University, Yangzhou 225127, China

* **Correspondence:** Email: dengweiwei_1994@163.com.

Abstract: This paper presents a new prescribed performance-based finite-time adaptive tracking control scheme for a class of pure-feedback nonlinear systems with input quantization and dynamical uncertainties. To process the input signal, a new quantizer combining the advantages of a hysteresis quantizer and uniform quantizer has been used. Radial basis function neural networks have been utilized to approximate unknown nonlinear smooth functions. An auxiliary system has been employed to estimate unmodeled dynamics by producing a dynamic signal. By introducing a hyperbolic tangent function and performance function, the tracking error was made to fall within the prescribed time-varying constraints. Using modified dynamic surface control (DSC) technology and a finite-time control method, a novel finite-time controller has been designed, and the singularity problem of differentiating each virtual control scheme in the existing finite-time control scheme has been removed. Theoretical analysis shows that all signals in the closed-loop system are semi-globally practically finite-time stable , and that the tracking error converges to a prescribed time-varying region. Simulation results for two numerical examples have been provided to illustrate the validity of the proposed control method.

Keywords: prescribed performance; dynamic surface control; finite-time stability; unmodeled dynamics; input quantization
Mathematics Subject Classification: 93A30, 93C10, 97N40

1. Introduction

Numerous nonlinear challenges arise in the realms of production and societal life, rendering conventional linear control theories and methods inadequate as tools to address these nonlinear control issues. Since Kanellakopoulos et al. [1] and Swaroop et al. [2] put forward the backstepping and dynamic surface control (DSC) design, the two design methods have been widely used in the

controller design of nonlinear systems [3–5]. In contrast to backstepping design, DSC offers a simpler alternative, circumventing the issue of over-parameterization that is often associated with conventional backstepping and streamlining the overall controller design process.

Unmodeled dynamics are prevalent in practical production and daily life. Modeling errors often arise during the system modeling process, leading to adverse effects on system stability [6–8]. In the work of Jiang and Praly [9], unmodeled dynamics was estimated by using measurable dynamic signals, and the assumption that unmodeled dynamics was exponentially input-state-practically stable (exp-ISpS). The work conducted by Hua and Zhang [10] effectively addressed a category of strict feedback systems that are characterized by unmodeled dynamics and time-varying full-state constraints through the application of the DSC technique. This approach demonstrated exceptional dynamic performance when handling complex system dynamics and evolving state limitations. In the work of Zhang et al. [11], a dynamic signal was introduced to deal with the dynamical uncertainties associated with adaptive output feedback systems with output constraints and unmodeled dynamics. In the work of Zhang et al. [12], the dynamic signals generated by the auxiliary system were used to process unmodeled dynamics for a class of strict-feedback nonlinear systems with full state constraints. In [13], adaptive triggered control for multiple input multiple output (MIMO) systems with unmodeled dynamics and output constraints was proposed in the work by Hua and Zhang. A class of pure-feedback systems with unmodeled dynamics were studied in the work by Zhang and Lin [14]. References [9–14] extensively discuss the impact of unmodeled dynamics on the system. However, it is noteworthy that these references do not explicitly consider the influence of input quantization on the overall system.

Signal quantization involves the transformation of a continuous signal into a discrete signal with a limited set of values after passing through a quantizer [15, 16]. In advanced fields such as medical, aerospace, and military applications, the application of quantization control has become increasingly prevalent. The accurate and efficient quantification of signals plays a crucial role in the advancement of quantitative control methodologies. To date, substantial research efforts have been dedicated to the study of input quantization, illuminating its significance in various domains and the need for robust and effective quantization techniques. So far, there are many studies researches on input quantification. In [17], a class of nonlinear systems with quantization time delay was studied. Under the assumption that the sector region of the quantizer was bounded, the stability problem of strict-feedback nonlinear systems with state quantization was studied in the work of Liu et al. [18]. Combining the advantages of the hysteresis quantizer and uniform quantizer, Xing et al. proposed a new quantizer, which is an extension of the existing quantizer [19]. In the works of Xia and Zhang [20], a novel controller compensation was designed to eliminate the influence of input quantization on the system. On the basis of the results from previous works [20], in [21], to simplify the difficulty of controller design, the quantizer error was further linearized. References [22, 23] primarily focus on addressing a specific category of input quantization problems within the context of finite-time control.

Finite-time control has witnessed substantial advancements in recent decades [24, 25]. A defining characteristic of finite-time control is its ability to bring the system's state to equilibrium within a finite duration, after which the system remains in equilibrium. In the work of Bhat and Bernstein [26, 27], the Lyapunov theory and homogeneous system theory of finite-time stability were first proposed, and the flutter phenomenon caused by the controller was solved. On this basis, many finite-time stability problems of nonlinear systems were discussed. In the works of Chen and Yang [28] and Yang and Sun [29], the finite-time stability of time-varying delay systems was successfully addressed

through the application of Lyapunov-Krasovskii functions. However, it is important to note that the discussions in these works did not cover specified performance and input quantization aspects. In the work of Liu et al. [30], the finite-time control methods of nonlinear systems were systematically and perfectly presented. The finite-time problem was investigated for a class of strict-feedback nonlinear systems in the work of Li et al. [31]. References [32, 33] predominantly delve into finite-time control methodologies applied to diverse systems by using the backstepping design. It is worth noting that, while effective, the backstepping technique can give rise to computational complexity issues [34–36]. Additionally, the virtual control law is derived repetitively in the virtual control design, leading to an increase in the structural complexity of the controller as the system's order rises. As a result, addressing these challenges becomes imperative for the widespread applicability and scalability of finite-time control techniques. References [37, 38] adopted DSC to avoid the "complexity" problem in conventional backstepping, and they brought about new ideas for the design of finite-time controllers. MIMO non-strict feedback systems were studied, but they still had the problem of singularity in the work. Reference [38] adopted a DSC method and presented a new form of first-order filter. However, the symbolic function was used in the design of the virtual controller, which made the virtual control law non-differentiable and led to theoretical errors in the following process. In a study conducted by Liu et al. [39], the investigation focused on finite-time control for nonlinear systems. Notably, Young's inequality was employed as a substitute for a conventional inequality theorem commonly found in the finite-time literature. This innovative approach aimed to enhance the efficiency and analytical tractability of finite-time control methodologies in the context of nonlinear systems.

The prescribed performance function (PPF) requires that the system satisfies the conditions for instantaneity and stability performance. In the research conducted by Liu et al. [40], an adaptive PPF tracking controller was formulated, leveraging the backstepping technique as its foundational design methodology. By using the properties of the bounds of the hyperbolic tangent function, the error transformation was carried out, which provided a new idea for the study of PPFs in the work of Shi [41]. Xia et al. [42] used linear mapping to transform the error and realized the prescribed performance tracking control.

Inspired by the above literature, this paper focuses on the finite-time adaptive prescribed performance DSC for pure-feedback nonlinear systems featuring unmodeled dynamics and input quantization. A novel control strategy is proposed, and the primary contributions can be summarized as follows:

(1) This paper introduces a novel finite-time adaptive tracking control scheme for a specific class of pure-feedback nonlinear systems characterized by input quantization and dynamical uncertainties. A hybrid quantizer, amalgamating the advantages of a hysteresis quantizer and a uniform quantizer, is employed to address the input signal.
(2) The proposed control scheme incorporates the hyperbolic tangent function and a performance function to ensure that the tracking error adheres to prescribed time-varying constraints. The singularity problem of differentiating each virtual control in the existing finite-time control scheme [22, 32, 37] is removed by constructing an appropriate unknown continuous function at each step of recursion.
(3) Theoretical analysis demonstrates the semi-global practical finite-time stability (SGPFTS) of all signals in the closed-loop system, with the tracking error converging to a prescribed time-varying region. To validate the efficacy of the proposed control method, simulation results from

two numerical examples are provided, illustrating its applicability and robustness in real-world scenarios.

The remaining sections of this paper are organized as follows. Section 2 provides the problem statement and some preparatory work, such as radial basis function (RBF) neural networks and quantization design. Sections 3 and 4 present the error transformation and adaptive controller design. Section 5 outlines the main results of this paper. The portion based on MATLAB/SIMULINK is covered in Section 6. Finally, the conclusion and prospects for future work are discussed in Section 7.

2. Problem statement and preliminaries

Consider the following pure-feedback nonlinear systems

$$\begin{cases} \dot{\hbar} = Q(\hbar, x, t), \\ \dot{x}_i = f_i(\bar{x}_i, x_{i+1}) + d_i(\hbar, x, t), \quad i = 1, \ldots, n, \\ \dot{x}_n = f_n(\bar{x}_n) + q(u) + d_n(\hbar, x, t), n \geq 2, \\ y = x_1, \end{cases} \tag{2.1}$$

where $\bar{x}_i = [x_1, ..., x_i]^T \in R^i (i = 1, 2, ..., n)$ denotes the state vectors of system (2.1); $\hbar \in R^{n_0}$ represents the unmodeled dynamics; $Q(\hbar, x, t)$ is an unknown Lipschitz function; $y \in R$ represents the system output; $u \in R$ is the control input; $f_i(\bar{x}_i)$ denotes an unknown smooth function; $q(u)$ is the quantized signal, and $d_i(\hbar, x, t)$ is the unknown disturbance.

The control objective is to design a controller u and quantizer $q(u)$ so that the output can track the desired trajectory and the tracking error can converge to a preset area in finite-time. Meanwhile, all signals of the closed-loop system exhibit SGPFTS.

Definition 1. *[9] For system $\dot{\hbar} = Q(\hbar, x, t)$, if there exist functions $\bar{\alpha}_1$ and $\bar{\alpha}_2$ of class K_∞ and a Lyapunov function $V_0(\xi)$ such that*

$$\bar{\alpha}_1(\|\hbar\|) \leq V_0(\hbar) \leq \bar{\alpha}_2(\|\hbar\|) \tag{2.2}$$

and if there exist two known constants $c > 0$, $d \geq 0$ and a class K_∞ function $\Lambda(\cdot)$ such that

$$\frac{\partial V_0(\hbar)}{\partial \hbar} Q(\hbar, x, t) \leq -cV_0(\hbar) + \Lambda(|x_1|) + d \tag{2.3}$$

then the unmodeled dynamics is said to be exp-ISpS.

Assumption 1. *[11] The desired trajectory vector satisfies the $x_d = [y_d, \dot{y}_d, \ddot{y}_d]^T \in \Omega_d$, where $\Omega_d = \{x_d : y_d^2 + \dot{y}_d^2 + \ddot{y}_d^2 \leq B_0\}$, $|y_d| \leq B_1$, and B_0, B_1 are known positive constants.*

Assumption 2. *[20] For unknown disturbance $d_i(\xi, x, t)$, $i = 1, 2, ..., n$, there are an unknown non-negative continuous function $\Delta_{i1}(\cdot)$ and an unknown non-negative continuous monotonic increasing function $\Delta_{i2}(\cdot)$ satisfying the following inequality:*

$$|d_i(\hbar, x, t)| \leq \Delta_{i1}(\|\bar{x}_i\|) + \Delta_{i2}(\|\hbar\|) \tag{2.4}$$

where $i = 1, 2 \ldots n$ and $\|\cdot\|$ stands for the Euclidean norm of a vector or the 2-norm of a matrix.

Lemma 1. *[9] If $V_0(\xi)$ is an exp-ISpS Lyapunov function for a system $\dot{\hbar} = Q(\hbar, x, t)$, then, for any constants $\bar{c}_f \in (0, c)$, the initial condition $\hbar_0 = \hbar(t_0)$ and $r_0 > 0$. For any continuous function $\bar{\Lambda}$ such that $\bar{\Lambda}(|x_1|) \geq \Lambda(|x_1|)$, there exist a finite $T_0 = \max\left\{0, \ln\left[V_0(\hbar_0)/r_0\right]/\left(c - \bar{c}_f\right)\right\} \geq 0$, a non-negative function $D(t_0, t)$, defined for all $t \geq t_0$, and a signal described by*

$$\dot{r} = -\bar{c}_f r + \bar{\Lambda}(|x_1|) + d \tag{2.5}$$

such that $D(t_0, t) = 0$ for $t \geq t_0 + T_0$ and $V_0(\hbar) \leq r(t) + D(t_0, t)$. Without loss of generality, $\bar{\Lambda}(|x_1|) = \Lambda(|x_1|)$.

Lemma 2. *[43] For the nonlinear system $\dot{x} = f(x)$, if there exist a positive definite C^1 functions $V(x) : R^n \to R$, a compact set $\Sigma \subset R^n$, class K_∞ functions ς_1, ς_2, and some scalars $\alpha > 0, \frac{1}{2} \leq q < 1, 0 < C < \infty, 0 < v < 1$, and $0 < \beta < 1$, for any $x(t_0) = x_0 \in \Sigma$ such that $\varsigma_1(\|x\|) \leq V(x) \leq \varsigma_2(\|x\|)$ and the solution of $\dot{x} = f(x)$ with initial value $x(t_0) = x_0 \in \Sigma$ satisfies*

$$\dot{V}(x) \leq -\alpha V(x) - \beta V^q(x) + C \tag{2.6}$$

then the nonlinear system $\dot{x} = f(x)$ exhibits SGPFTS for the setting time

$$T_r = t_0 + \frac{1}{\alpha(1-q)} \ln \frac{\alpha V^{1-q}(x_0) + v\beta}{v\beta}.$$

Lemma 3. *[38] For any $\eta_1, \ldots, \eta_N \in R^+$ and $0 < s \leq 1$, then*

$$\left(\sum_{i=1}^{N} \eta_i\right)^s \leq \sum_{i=1}^{N} \eta_i^s \leq N^{1-s} \left(\sum_{i=1}^{N} \eta_i\right)^s. \tag{2.7}$$

Lemma 4 (Young's inequality)**.** *[37] If $\forall \varphi, \psi \in R, \varepsilon > 0, a > 1, b > 1$, and $\frac{1}{a} + \frac{1}{b} = 1$, then the following inequality holds:*

$$|\varphi\psi| \leq \frac{\varepsilon^a}{a}|\varphi|^a + \frac{1}{b\varepsilon^b}|\psi|^b. \tag{2.8}$$

Particularly, when $a = 2$, $b = 2$, and $\varepsilon = 1$, we have that $\varphi\psi \leq \frac{1}{2}\varphi^2 + \frac{1}{2}\psi^2$; when $a = 2$, $b = 2$, and $\varepsilon = \frac{1}{\sqrt{2}}$, we have that $\varphi\psi \leq \frac{1}{4}\varphi^2 + \psi^2$.

2.1. Radial basis function neural networks

Using radial basis function neural networks $\theta_i^{*T}\phi_i(Z_i)$ to approximate the continuous function $\Phi_i(Z_i)$ on the compact set Π_{Z_i}, then

$$\Phi_i(Z_i) = \theta_i^{*T}\phi_i(Z_i) + \varepsilon_i(Z_i), \tag{2.9}$$

where $Z_1 = \left[\bar{x}_2^T, z_1, y_d, \dot{y}_d, \varpi, \dot{\varpi}, k_c(t), \dot{k}_c(t), r\right]^T$, $Z_i = \left[\bar{x}_{i+1}^T, z_i, y_i, r\right]^T$, $i = 2, \ldots, n$, the basis function vectors $\phi_i(Z_i) = \left[\varphi_{i1}(Z_i), \ldots, \varphi_{il_i}(Z_i)\right]^T \in R^{l_i}$, and the basis functions $\varphi_{i,j}(Z_i)$ are selected as Gaussian functions as follows:

$$\varphi_{i,j}(Z_i) = e^{-\frac{\left(Z_i - \mu_{ij}\right)^T \left(Z_i - \mu_{ij}\right)}{\phi_{ij}^2}}. \tag{2.10}$$

ϕ_{ij} and μ_{ij} are respectively, the width and center of the Gaussian functions, and $i = 1, \ldots, n$; $j = 1, \ldots, l_i$, l_i is the number of nodes of the neural networks. The ideal weights θ_i^* are defined as follows:

$$\theta_i^* = \arg\min_{\theta_i \in R^{l_i}} \left[\sup_{Z_i \in \Omega_{Z_i}} \left|\theta_i^T \phi_i(Z_i) - \Phi_i(Z_i)\right|\right]. \tag{2.11}$$

2.2. Quantizer design

In this paper, a new quantizer that combines a hysteresis quantizer with a uniform quantizer not only avoids quantization signal chatter, it also keeps the upper bound of quantization error constant. The new quantizer was proposed by Wang et al. [21], and it is described as follows:

$$q(u) = \begin{cases} q_h(u_{th}) + Int\left[\frac{u-u_{th}}{\bar{v}} + \kappa(u_{th})\right]\bar{v}, & |u| \geq u_{th}, \\ q_h(u), & |u| < u_{th}, \end{cases} \tag{2.12}$$

where

$$q_h(u) = \begin{cases} u_i \mathrm{sgn}(u), & \frac{u_i}{1+\delta} < |u| < u_i, \dot{u} < 0, or \\ & u_i < |u| \leq \frac{u_i}{1-\delta}, \dot{u} > 0, \\ u_i(1+\delta)\mathrm{sgn}(u), & u_i < |u| \leq \frac{u_i}{1-\delta}, \dot{u} < 0, or \\ & \frac{u_i}{1-\delta} < |u| < \frac{u_i(1+\delta)}{1-\delta}, \dot{u} > 0, \\ 0, & 0 \leq |u| < \frac{u_{\min}}{1+\delta}, or \\ & \frac{u_{\min}}{1+\delta} < |u| \leq u_{\min}, \dot{u} > 0, \\ q_h(u(t^-)), & \dot{u} = 0, \end{cases} \tag{2.13}$$

$$\kappa(u_{th}) = \begin{cases} 1, & q_h(u_{th}) < u_{th}, \\ 0, & q_h(u_{th}) \geq u_{th}. \end{cases} \tag{2.14}$$

$u_i = p^{1-i}u_{\min}, i = 1, 2, \ldots n$, $u_{\min} > 0$ and $0 < p < 1$ determine the quantization density of $q_h(u)$ and $\delta = \frac{1-p}{1+p}$, $q_h(u)$ is in the set $U = \{0, \pm u_i, \pm u_i(1+\delta)\}$. $Int[d]$ stands for the maximum integer which is less than or equal to d. The design parameter $\bar{v} \geq |q_h(u_{th}) - u_{th}|$ determines the quantization density of the uniform quantizer, u_{th} which is a designed normal number and the threshold for switching between two quantizers. The quantization error can be obtained by the new quantizer as follows:

$$\left|\Delta_q\right| \leq \begin{cases} \bar{v}, |u| \geq u_{th}, \\ \delta u_{th} + (1-\delta)u_{\min}, |u| < u_{th}. \end{cases} \tag{2.15}$$

It is obvious that the quantization error Δ_q of the new quantizer is bounded for any u, and that there exists a positive constant d such that $\left|\Delta_q\right| \leq d$, where $d = \max\{\bar{v}, \delta u_{th} + (1-\delta)u_{\min}\}$. According to $\Delta_q(u) = q(u) - u$, we can conclude that

$$q(u) = u + \Delta_q(u). \tag{2.16}$$

3. Error transformation

Define the PPF $\varpi(t)$ as follows:

$$\varpi(t) = (\varpi_0 - \varpi_\infty)\, e^{-k_0 t} + \varpi_\infty \tag{3.1}$$

where $\varpi(t)$ is a positive decreasing smooth function, and ϖ_0, ϖ_∞ and k_0 are the positive constants.

The tracking error is defined as follows:

$$e_1 = y - y_d. \tag{3.2}$$

In this section, the control signal u is designed to make the following inequality hold:

$$-k_c(t)\varpi < e_1 < k_c(t)\varpi \tag{3.3}$$

According to the control target in this paper, the tracking error is in the prescribed region described by Eq (3.3).

Let

$$S = \frac{1}{2}\log\frac{k_c(t)+\frac{e_1}{\varpi}}{k_c(t)-\frac{e_1}{\varpi}}. \tag{3.4}$$

Inverse transformation of the coordinates is given as

$$\frac{e_1}{\varpi} = k_c(t)\tanh S. \tag{3.5}$$

Then

$$\dot{S} = \frac{1}{k_c(t)\varpi\left(1-\tanh^2 S\right)}\dot{e}_1 - \frac{e_1\dot{\varpi}}{\varpi^2 k_c(t)\left(1-\tanh^2 S\right)} - \frac{\dot{k}_c(t)\tanh S}{k_c(t)\left(1-\tanh^2 S\right)}. \tag{3.6}$$

Let

$$m(t) = \frac{1}{k_c(t)\varpi\left(1-\tanh^2 S\right)} > 0, \tag{3.7}$$

$$n(t) = -\frac{e_1\dot{\varpi}}{\varpi^2 k_c(t)\left(1-\tanh^2 S\right)} - \frac{\dot{k}_c(t)\tanh S}{k_c(t)\left(1-\tanh^2 S\right)}. \tag{3.8}$$

Therefore, Eq (3.6) can be rewritten as follows:

$$\dot{S} = m(t)\dot{e}_1 + n(t). \tag{3.9}$$

4. Adaptive control design

Let $F_i(\bar{x}_{i+1}) = f_i(\bar{x}_i, x_{i+1}) - x_{i+1}$, $i = 1,\ldots,n-1$, $F_n(\bar{x}_n) = f_n(\bar{x}_n)$; then, system (2.1) can be changed into the following form:

$$\begin{cases} \dot{\hbar} = \mathrm{Q}(\hbar, x, t), \\ \dot{x}_i = F_i(\bar{x}_{i+1}) + x_{i+1} + d_i(\hbar, x, t), \\ \dot{x}_n = F_n(\bar{x}_n) + q(u) + d_n(\hbar, x, t), \\ y = x_1. \end{cases} \tag{4.1}$$

To facilitate the controller design, the following coordinate changes are introduced:

$$\begin{cases} z_1 = S, \\ z_i = x_i - \omega_i, i = 2,\ldots,n. \end{cases} \tag{4.2}$$

where ω_i is the output of the nonlinear filter with input $\hbar_{i-1}, i = 2,\ldots,n$.

Define some symbols as follows: $sig(\cdot)^{\vartheta} = |\cdot|^{\vartheta}\mathrm{sgn}(\cdot)$, $\lambda_i = \left\|\theta_i^*\right\|^2$, $\tilde{\lambda}_i = \hat{\lambda}_i - \lambda_i$, $\bar{z}_i = [z_1,\ldots,z_i]^T$, $\bar{y}_j = \left[y_2,\ldots,y_j\right]^T$, $\overline{\hat{\lambda}}_i = \left[\hat{\lambda}_1,\ldots,\hat{\lambda}_i\right]^T$, $1 \le i \le n, 2 \le j \le n$, where $\hat{\lambda}_i$ denotes the estimation of λ_i, $y_j = \omega_j - \hbar_{j-1}$.

Step 1. Define the first dynamic surface as follows:

$$z_1 = S. \tag{4.3}$$

The time derivative of z_1 is given by

$$\dot{z}_1 = m(t)\left(F_1\left(\bar{x}_2\right) + y_2 + z_2 + \hbar_1 + d_1(t, \hbar, x) - \dot{y}_d\right) + n(t). \tag{4.4}$$

Select $V_1 = \frac{1}{2}z_1^2 + \frac{1}{2}\tilde{\lambda}_1^2$ as the Lyapunov function; the time derivative of V_1 is given by

$$\dot{V}_1 = z_1\left[m(t)\left(F_1\left(\bar{x}_2\right) + y_2 + z_2 + \hbar_1 + d_1(t, \hbar, x) - \dot{y}_d\right) + n(t)\right] + \tilde{\lambda}_1\dot{\tilde{\lambda}}_1. \tag{4.5}$$

Using Lemmas 1 and 4 and Assumption 2, it follows that

$$\begin{aligned} z_1 m(t) d_1(t, \hbar, x) &\leq z_1 m(t)[\Delta_{11}(|x_1|) + \Delta_{12}(\|\hbar\|)] \\ &\leq z_1^2 m^2[\Delta_{11}(|x_1|) + \Delta_{12} \circ \bar{\alpha}_1(r + D_0)]^2 + \frac{1}{4}, \end{aligned} \tag{4.6}$$

$$z_1 z_2 m(t) \leq \frac{1}{4}z_1^2 m^2 + z_2^2, \tag{4.7}$$

$$z_1 y_2 m(t) \leq \frac{1}{4}z_1^2 m^2 + y_2^2. \tag{4.8}$$

Substituting Eqs (4.6)–(4.8) into Eq (4.5), we have

$$\begin{aligned} \dot{V}_1 \leq & z_1[m(F_1(\bar{x}_2) + \hbar_1 - \dot{y}_d + z_1 m[\Delta_{11}(|x_1|) + \Delta_{12} \circ \bar{\alpha}_1(r + D_0)]^2 \\ & + n(t)] + \tilde{\lambda}_1\dot{\tilde{\lambda}}_1 + \frac{1}{4} + \frac{1}{2}m^2 z_1^2 + y_2^2 + z_2^2. \end{aligned} \tag{4.9}$$

Let

$$\Phi_1\left(Z_1\right) = mF_1\left(\bar{x}_2\right) - m\dot{y}_d + z_1 m^2\left[\Delta_{11}\left(|x_1|\right) + \Delta_{12} \circ \bar{\alpha}_1\left(r + D_0\right)\right]^2 + n(t) + |z_1|^{2q-1}$$

where $Z_1 = \left[\bar{x}_2^T, z_1, y_d, \dot{y}_d, \varpi, \dot{\varpi}, k_c(t), \dot{k}_c(t), r\right]^T$ and $0.5 \leq q < 1$; then,

$$\dot{V}_1 \leq z_1\left[\theta_1^{*T}\phi_1\left(Z_1\right) + m\hbar_1 - |z_1|^{2q-1}\right)\Big] + z_1\varepsilon_1 + \tilde{\lambda}_1\dot{\tilde{\lambda}}_1 + \frac{1}{4} + \frac{1}{2}m^2 z_1^2 + y_2^2 + z_2^2. \tag{4.10}$$

Using Young's inequality yields

$$z_1\theta_1^{*T}\phi_1\left(Z_1\right) \leq \frac{\|\phi_1\left(Z_1\right)\|^2 z_1^2\lambda_1}{2a_1^2} + \frac{a_1^2}{2} \tag{4.11}$$

where a_1 is a positive constant.

Therefore, Eq (4.10) can be rewritten as follows:

$$\dot{V}_1 \leq z_1\left(\frac{\|\phi_1(Z_1)\|^2 z_1\lambda_1}{2a_1^2} + m\hbar_1 - |z_1|^{2q-1}\right) + \tilde{\lambda}_1\dot{\tilde{\lambda}}_1 + \frac{1}{4} + \frac{1}{2}m^2 z_1^2 + y_2^2 + z_2^2 + \frac{a_1^2}{2} + z_1\varepsilon_1. \tag{4.12}$$

The virtual control law is constructed as follows:

$$\hbar_1 = -\frac{1}{m}((k_1 + 1 + \frac{1}{2}m^2)z_1 + \frac{\|\phi_1(Z_1)\|^2 z_1 \hat{\lambda}_1}{2a_1^2}). \tag{4.13}$$

Design the adaptive law of $\hat{\lambda}_1$ as follows:

$$\dot{\hat{\lambda}}_1 = \frac{\|\phi_1(Z_1)\|^2 z_1^2}{2a_1^2} - \sigma_1 \hat{\lambda}_1, \tag{4.14}$$

where k_1, a_1 are positive design constants.

Substituting Eqs (4.13) and (4.14) into Eq (4.12), we have

$$\dot{V}_1 \leq -k_1 z_1^2 - |z_1|^{2q} + y_2^2 + z_2^2 - \sigma_1 \tilde{\lambda}_1 \hat{\lambda}_1 + \frac{a_1^2}{2} + \frac{1}{4} - z_1^2 + z_1 \varepsilon_1. \tag{4.15}$$

The non-negative continuous function $\delta_1(\bar{z}_2, \hat{\lambda}_1, y_d, \dot{y}_d, y_2, r, k_c(t), \dot{k}_c(t))$ satisfies

$$|\varepsilon_1(Z_1)| \leq \delta_1(\bar{z}_2, \hat{\lambda}_1, y_d, \dot{y}_d, y_2, r, k_c(t), \dot{k}_c(t)).$$

Based on Young's inequality, we further get

$$z_1 \varepsilon_1 \leq z_1^2 + \frac{1}{4}\delta_1^2, \tag{4.16}$$

$$-\sigma_1 \tilde{\lambda}_1 \hat{\lambda}_1 \leq -\frac{\sigma_1}{2}\tilde{\lambda}_1^2 + \frac{\sigma_1}{2}\lambda_1^2 \leq -\sigma_1 \frac{1-q}{2}\tilde{\lambda}_1^2 + \frac{\sigma_1}{2}\lambda_1^2 - \sigma_1 \frac{q}{2}\tilde{\lambda}_1^2. \tag{4.17}$$

Therefore, we obtain

$$\dot{V}_1 \leq -k_1 z_1^2 - |z_1|^{2q} + y_2^2 + z_2^2 - \sigma_1 \frac{1-q}{2}\tilde{\lambda}_1^2 + \frac{\sigma_1}{2}\lambda_1^2 - \sigma_1 \frac{q}{2}\tilde{\lambda}_1^2 + \frac{a_1^2}{2} + \frac{1}{4} + \frac{1}{4}\delta_1^2. \tag{4.18}$$

Let $x = \tilde{\lambda}_1^{2q}, y = 1, a = \frac{1}{q} > 1$, and $b = \frac{1}{1-q}$. According to Lemma 4, we obtain

$$\tilde{\lambda}_1^{2q} \leq q\left(\tilde{\lambda}_1^{2q}\right)^{\frac{1}{q}} + (1-q) = q\tilde{\lambda}_1^2 + (1-q). \tag{4.19}$$

Therefore

$$-\frac{\sigma_1 q \tilde{\lambda}_1^2}{2} \leq -\frac{\sigma_1 \tilde{\lambda}_1^{2q}}{2} + \frac{\sigma_1(1-q)}{2}. \tag{4.20}$$

Substituting Eq (4.20) into Eq (4.15), we have

$$\begin{aligned} \dot{V}_1 \leq & -k_1 z_1^2 - |z_1|^{2q} + y_2^2 + z_2^2 - \sigma_1 \frac{1-q}{2}\tilde{\lambda}_1^2 + \frac{\sigma_1}{2}\lambda_1^2 - \frac{\sigma_1 \tilde{\lambda}_1^{2q}}{2} \\ & + \frac{\sigma_1(1-q)}{2} + \frac{a_1^2}{2} + \frac{1}{4} + \frac{1}{4}\delta_1^2. \end{aligned} \tag{4.21}$$

Inspired by Li et al. in [38], the nonlinear filter ω_2 is designed as follows:

$$\tau_2 \dot{\omega}_2 = \operatorname{sig}(\hbar_1 - \omega_2)^{2q-1} + \operatorname{sig}(\hbar_1 - \omega_2), \tag{4.22}$$

i.e.,

$$-\dot{\omega}_2 = \frac{1}{\tau_2}|y_2|^{2q-1}\,\mathrm{sgn}\,(y_2) + \frac{1}{\tau_2}|y_2|\,\mathrm{sgn}\,(y_2) \le \frac{1}{\tau_i^2}|y_2|^{4q-2} + \frac{1}{\tau_2^2}y_2^2 + \frac{1}{2}.$$

where $\hbar_1$ and ω_2 are the input and output of the filter, respectively, and τ_2 is a positive constant.

Step 2. ($2 \le i \le n-1$). Since $z_i = s_i - \omega_i$, the time derivative of z_i is given by

$$\dot{z}_i = F_i(\bar{x}_{i+1}) + y_{i+1} + z_{i+1} + \hbar_i - \dot{\omega}_i + d_i(t,\hbar,x). \tag{4.23}$$

Choose $V_i = V_{i-1} + \frac{1}{2}z_i^2 + \frac{1}{2}\tilde{\lambda}_i^2 + \frac{1}{2}y_i^2$; the time derivative of V_i can be obtained as follows

$$\begin{aligned}\dot{V}_i &= \dot{V}_{i-1} + z_i\dot{z}_i + \tilde{\lambda}_i\dot{\tilde{\lambda}}_i + y_i\dot{y}_i \\ &= \dot{V}_{i-1} + z_i\left[F_i(\bar{x}_{i+1}) + y_{i+1} + z_{i+1} + \hbar_i - \dot{\omega}_i + d_i(t,\hbar,x)\right] + \tilde{\lambda}_i\dot{\tilde{\lambda}}_i + y_i\dot{y}_i.\end{aligned} \tag{4.24}$$

Substituting Eq (4.22) into Eq (4.24), we obtain

$$\begin{aligned}\dot{V}_i =& \dot{V}_{i-1} + z_i\dot{z}_i + \tilde{\lambda}_i\dot{\tilde{\lambda}}_i + y_i\dot{y}_i \\ =& \dot{V}_{i-1} + z_i\left[F_i(\bar{x}_{i+1}) + y_{i+1} + z_{i+1} + \hbar_i + d_i(t,\hbar,x) + \frac{1}{\tau_i^2}|y_i|^{4p-2} + \frac{1}{\tau_i^2}y_i^2 + \frac{1}{2}\right] + \tilde{\lambda}_i\dot{\tilde{\lambda}}_i + y_i\dot{y}_i.\end{aligned} \tag{4.25}$$

From Assumption 2 and Lemma 1, and by using Young's inequality, we get

$$z_i d_i(t,\hbar,\bar{s}_n) \le z_i\left[\Delta_{i1}(\|\bar{x}_i\|) + \Delta_{i2}(\|\hbar\|)\right] \le z_i^2\left[\Delta_{i1}(\|\bar{x}_i\|) + \Delta_{i2}\circ\bar{\alpha}_1^{-1}(r+D_0)\right]^2 + \frac{1}{4}, \tag{4.26}$$

$$z_i z_{i+1} \le \frac{1}{4}z_i^2 + z_{i+1}^2, \tag{4.27}$$

$$z_i y_{i+1} \le \frac{1}{4}z_i^2 + y_{i+1}^2. \tag{4.28}$$

From Eqs (4.26)–(4.28), we know that

$$\begin{aligned}\dot{V}_i \le& \sum_{j=1}^{i-1}\left[-k_j z_j^2 - |z_j|^{2q} - \frac{\sigma_j(1-q)}{2}\tilde{\lambda}_j^2 - \frac{\sigma_j}{2}\tilde{\lambda}_j^{2q}\right] \\ &+ \sum_{j=1}^{i-1}\left[\frac{1}{4}\delta_j^2 + \frac{1}{2}a_j^2 + \frac{\sigma_j}{2}\lambda_j^2 + \frac{j}{4} + \frac{\sigma_j(1-q)}{2}\right] \\ &+ \sum_{j=2}^{i-1}\left[-\frac{1}{\tau_j}y_j^{2q} - \left(\frac{1}{\tau_j} - 2\right)y_j^2 + \frac{1}{4}\eta_j^2\right] + \frac{3}{2}z_i^2 + y_i^2 + z_i\left[F_i(\bar{x}_{i+1}) + y_{i+1} + z_{i+1}\right. \\ &\left.+\hbar_i + \frac{1}{\tau_i^2}|y_i|^{4p-2} + \frac{1}{\tau_i^2}y_i^2 + \frac{1}{2} + z_i\left(\Delta_{i1}(\|\bar{x}_i\|) + \Delta_{i2}\circ\bar{\alpha}_1^{-1}(r+D_0)\right)^2\right] \\ &+ \tilde{\lambda}_i\dot{\tilde{\lambda}}_i + y_i\dot{y}_i + z_{i+1}^2 + y_{i+1}^2 + \frac{1}{4}.\end{aligned} \tag{4.29}$$

Let

$$\begin{aligned}\Phi_i(Z_i) =& F_i(\bar{x}_{i+1}) + y_{i+1} + z_{i+1} + |z_i|^{2q-1} \\ &+ \frac{1}{\tau_i^2}|y_i|^{4p-2} + \frac{1}{\tau_i^2}y_i^2 + \frac{1}{2} + z_i\left[\Delta_{i1}(\|\bar{x}_i\|) + \Delta_{i2}\circ\bar{\alpha}_1(r+D_0)\right]^2,\end{aligned}$$

where $Z_i = \left[\bar{x}_{i+1}^T, z_i, y_i, r\right]^T$. Therefore, we have

$$\begin{aligned}\dot{V}_i \leq & \sum_{j=1}^{i-1}\left[-k_j z_j^2 - \left|z_j\right|^{2q} - \frac{\sigma_j(1-q)}{2}\tilde{\lambda}_j^2 - \frac{\sigma_j}{2}\tilde{\lambda}_j^{2q}\right] \\ & + \sum_{j=1}^{i-1}\left[\frac{1}{4}\delta_j^2 + \frac{1}{2}a_j^2 + \frac{\sigma_j}{2}\lambda_j^2 + \frac{j}{4} + \frac{\sigma_j(1-q)}{2}\right] \\ & + \sum_{j=2}^{i-1}\left[-\frac{1}{\tau_j}y_j^{2q} - \left(\frac{1}{\tau_j} - 2\right)y_j^2 + \frac{1}{4}\eta_j^2\right] + \frac{3}{2}z_i^2 + y_i^2 + \frac{1}{4} \\ & + z_i\left[\theta_i^{*T}\phi_i(Z_i) + \varepsilon_i + \hbar_i - |z_i|^{2q-1}\right] + \tilde{\lambda}_i\dot{\tilde{\lambda}}_i + y_i\dot{y}_i + z_{i+1}^2 + y_{i+1}^2.\end{aligned} \tag{4.30}$$

Using Young's inequality yields

$$z_i\theta_i^{*T}\phi_i(Z_i) \leq \frac{\left\|\phi_i(Z_i)\right\|^2 z_i^2\lambda_i}{2a_i^2} + \frac{a_i^2}{2}, \tag{4.31}$$

where $a_i > 0$ is a design constant.

Therefore, Eq (4.30) can be changed as follows:

$$\begin{aligned}\dot{V}_i \leq & \sum_{j=1}^{i-1}\left[-k_j z_j^2 - \left|z_j\right|^{2q} - \frac{\sigma_j(1-q)}{2}\tilde{\lambda}_j^2 - \frac{\sigma_j}{2}\tilde{\lambda}_j^{2q}\right] \\ & + \sum_{j=1}^{i-1}\left[\frac{1}{4}\delta_j^2 + \frac{1}{2}a_j^2 + \frac{\sigma_j}{2}\lambda_j^2 + \frac{j}{4} + \frac{\sigma_j(1-q)}{2}\right] + \frac{1}{4} \\ & + \sum_{j=2}^{i-1}\left[-\frac{1}{\tau_j}y_j^{2q} - \left(\frac{1}{\tau_j} - 2\right)y_j^2 + \frac{1}{4}\eta_j^2\right] + \frac{3}{2}z_i^2 + \frac{a_i^2}{2} \\ & + z_i\left[\frac{\left\|\phi_i(Z_i)\right\|^2 z_i\lambda_i}{2a_i^2} + \hbar_i - |z_i|^{2q-1}\right] + \tilde{\lambda}_i\dot{\tilde{\lambda}}_i + y_i\dot{y}_i + z_{i+1}^2 + z_i\varepsilon_i.\end{aligned} \tag{4.32}$$

Construct the virtual control law $\hbar_i$ as follows:

$$\hbar_i = -\left(k_i + \frac{5}{2}\right)z_i - \frac{\left\|\phi_i(Z_i)\right\|^2 z_i\hat{\lambda}_i}{2a_i^2}, \tag{4.33}$$

$$\dot{\hat{\lambda}}_i = \frac{\left\|\phi_i(Z_i)\right\|^2 z_i^2}{2a_i^2} - \sigma_i\hat{\lambda}_i, \tag{4.34}$$

where k_i, σ_i are positive design constants.

Substituting Eqs (4.33) and (4.34) into Eq (4.32), we have

$$\begin{aligned}\dot{V}_i \leq & \sum_{j=1}^{i}\left[-k_j z_j^2-\left|z_j\right|^{2q}-\frac{\sigma_j(1-q)}{2}\tilde{\lambda}_j^2-\frac{\sigma_j}{2}\tilde{\lambda}_j^{2q}\right] \\ & +\sum_{j=1}^{i}\left[\frac{1}{4}\delta_j^2+\frac{1}{2}a_j^2+\frac{\sigma_j}{2}\lambda_j^2+\frac{j}{4}+\frac{\sigma_j(1-q)}{2}\right]+y_i\dot{y}_i+z_{i+1}^2+y_{i+1}^2 \\ & +\sum_{j=2}^{i-1}\left[-\frac{1}{\tau_j}y_j^{2q}-\left(\frac{1}{\tau_j}-2\right)y_j^2+\frac{1}{4}\eta_j^2\right]+y_i^2-z_i^2+z_i\varepsilon_i+\sum_{j=1}^{i-1}\frac{1}{4}\delta_j^2.\end{aligned} \tag{4.35}$$

The non-negative continuous function $\delta_i\left(\bar{z}_{i+1},\bar{y}_{i+1},\overline{\hat{\lambda}}_i,y_d,\dot{y}_d,r\right)$ satisfies

$$\left|\varepsilon_i\left(Z_i\right)\right|\leq\delta_i\left(\bar{z}_{i+1},\bar{y}_{i+1},\overline{\hat{\lambda}}_i,y_d,\dot{y}_d,r\right).$$

Using Young's inequality yields

$$z_i\varepsilon_i\leq z_i^2+\frac{1}{4}\delta_i^2. \tag{4.36}$$

Therefore, we have

$$\begin{aligned}\dot{V}_i \leq & \sum_{j=1}^{i}\left[-k_j z_j^2-\left|z_j\right|^{2q}-\frac{\sigma_j(1-q)}{2}\tilde{\lambda}_j^2-\frac{\sigma_j}{2}\tilde{\lambda}_j^{2q}\right] \\ & +\sum_{j=1}^{i}\left[\frac{1}{4}\delta_j^2+\frac{1}{2}a_j^2+\frac{\sigma_j}{2}\lambda_j^2+\frac{j}{4}+\frac{\sigma_j(1-q)}{2}\right]+y_i\dot{y}_i+z_{i+1}^2+y_{i+1}^2 \\ & +\sum_{j=2}^{i-1}\left[-\frac{1}{\tau_j}y_j^{2q}-\left(\frac{1}{\tau_j}-2\right)y_j^2+\frac{1}{4}\eta_j^2\right]+y_i^2.\end{aligned} \tag{4.37}$$

Design a nonlinear filter ω_{i+1} as follows:

$$\dot{\omega}_{i+1}=\frac{1}{\tau_{i+1}}\operatorname{sig}\left(\hbar_i-\omega_{i+1}\right)^{2q-1}+\frac{1}{\tau_{i+1}}\operatorname{sig}\left(\hbar_i-\omega_{i+1}\right). \tag{4.38}$$

The nonnegative continuous function $\eta_{i+1}\left(\bar{z}_{i+2},\bar{y}_{i+2},\overline{\hat{\lambda}}_{i+1},y_d,\dot{y}_d,\ddot{y}_d,r,k_c(t),\dot{k}_c(t),\ddot{k}_c(t),\varpi,\dot{\varpi},\ddot{\varpi}\right)$ satisfies

$$\left|-\dot{\hbar}_i\right|\leq\eta_{i+1}\left(\bar{z}_{i+2},\bar{y}_{i+2},\overline{\hat{\lambda}}_{i+1},y_d,\dot{y}_d,\ddot{y}_d,r,k_c(t),\dot{k}_c(t),\ddot{k}_c(t),\varpi,\dot{\varpi},\ddot{\varpi}\right). \tag{4.39}$$

From Eqs (4.38) and (4.39, we obtain

$$\begin{aligned}y_{i+1}\dot{y}_{i+1}=y_{i+1}\left(\dot{\omega}_{i+1}-\dot{\hbar}_i\right)&=-\frac{1}{\tau_{i+1}}\left|y_{i+1}\right|^{2q}-\frac{1}{\tau_{i+1}}y_i^2-y_{i+1}\dot{\hbar}_i \\ &\leq-\frac{1}{\tau_{i+1}}\left|y_{i+1}\right|^{2q}-\frac{1}{\tau_{i+1}}y_{i+1}^2+y_{i+1}^2+\frac{1}{4}\eta_{i+1}^2.\end{aligned} \tag{4.40}$$

Therefore, we obtain

$$\begin{aligned}\dot{V}_i \leq & \sum_{j=1}^{i}\left[-k_j z_j^2 - \left|z_j\right|^{2q} - \frac{\sigma_j(1-q)}{2}\tilde{\lambda}_j^2 - \frac{\sigma_j}{2}\tilde{\lambda}_j^{2q}\right] \\ & + \sum_{j=1}^{i}\left[\frac{1}{4}\delta_j^2 + \frac{1}{2}a_j^2 + \frac{\sigma_j}{2}\lambda_j^2 + \frac{j}{4} + \frac{\sigma_j(1-q)}{2}\right] + z_{i+1}^2 + y_{i+1}^2 \\ & + \sum_{j=2}^{i}\left[-\frac{1}{\tau_j}y_j^{2q} - \left(\frac{1}{\tau_j} - 2\right)y_j^2 + \frac{1}{4}\eta_j^2\right].\end{aligned} \tag{4.41}$$

Step n. Since $z_n = s_n - \omega_n$, the time derivative of z_n is given by

$$\dot{z}_n = F_n(\bar{x}_n) + u + \Delta_q(u) + d_n(\hbar, x, t) - \dot{\omega}_n. \tag{4.42}$$

Let $V_n = V_{n-1} + \frac{1}{2}z_n^2 + \frac{1}{2}\tilde{\lambda}_n^2 + \frac{1}{2}y_n^2$; the time derivative of V_n is given by

$$\begin{aligned}\dot{V}_n &= \dot{V}_{n-1} + z_n\dot{z}_n + \tilde{\lambda}_n\dot{\tilde{\lambda}}_n + y_n\dot{y}_n \\ &= \dot{V}_{n-1} + z_n\left[F_n(\bar{x}_n) + u + \Delta_q(u) + d_n(\hbar, x, t) - \dot{\omega}_n\right] + \tilde{\lambda}_n\dot{\tilde{\lambda}}_n + y_n\dot{y}_n.\end{aligned} \tag{4.43}$$

Substituting Eq (4.42) into Eq (4.43), we obtain

$$\begin{aligned}\dot{V}_n \leq & \dot{V}_{n-1} + z_n\Big[F_n(\bar{x}_n) + u + \Delta_q(u) + d_n(\hbar, x, t) \\ & + \frac{1}{\tau_n^2}|y_n|^{4q-2} + \frac{1}{\tau_n^2}y_n^2 + \frac{1}{2}\Big] + \tilde{\lambda}_n\dot{\tilde{\lambda}}_n + y_n\dot{y}_n.\end{aligned} \tag{4.44}$$

From Assumption 2 and Lemma 1, and by using Young's inequality, we get

$$\begin{aligned}z_n d_n(t, \hbar, x) &\leq z_n\left[\Delta_{n1}(\|\bar{x}_n\|) + \Delta_{n2}(\|\hbar\|)\right] \\ &\leq z_n^2\left[\Delta_{n1}(\|\bar{x}_n\|) + \Delta_{n2} \circ \bar{\alpha}_1^{-1}(r + D_0)\right]^2 + \frac{1}{4}.\end{aligned} \tag{4.45}$$

$$z_n\Delta_q(u) \leq \frac{1}{2}z_n^2 + \frac{1}{2}d^2. \tag{4.46}$$

From Eqs (4.44)–(4.46), we know that

$$\begin{aligned}\dot{V}_n \leq & \dot{V}_{n-1} + z_n\Big\{F_n(\bar{x}_n) + u + \Delta_q(u) + z_n\left[\Delta_{n1}(\|\bar{x}_n\|) + \Delta_{n2} \circ \bar{\alpha}_1^{-1}(r + D_0)\right]^2 \\ & + \frac{1}{\tau_n^2}|y_n|^{4q-2} + \frac{1}{\tau_n^2}y_n^2 + \frac{1}{2}\Big\} + \tilde{\lambda}_n\dot{\tilde{\lambda}}_n + y_n\dot{y}_n + \frac{1}{4} + \frac{1}{2}z_n^2 + \frac{1}{2}d^2.\end{aligned} \tag{4.47}$$

Let

$$\begin{aligned}\Phi_n(Z_n) = & F_n(\bar{x}_n) + z_n\left[\Delta_{n1}(\|\bar{x}_n\|) + \Delta_{n2} \circ \bar{\alpha}_1(r + D_0)\right]^2 + |z_n|^{2q-1} \\ & + \frac{1}{\tau_n^2}|y_n|^{4q-2} + \frac{1}{\tau_n^2}y_n^2 + \frac{1}{2},\end{aligned}$$

where $Z_n = \left[\bar{x}_n^T, z_n, y_n, r\right]^T$.

Therefore, we have

$$\begin{aligned}\dot{V}_n \leq & \dot{V}_{n-1} + z_n\left(\theta_n^{*T}\phi_n(Z_n) + \varepsilon_n + u\right. \\ & \left. - |z_n|^{2q-1}\right) + \tilde{\lambda}_n\dot{\hat{\lambda}}_n + y_n\dot{y}_n + \frac{1}{4} + \frac{1}{2}z_n^2 + \frac{1}{2}d^2 \\ \leq & \sum_{j=1}^{n-1}\left[-k_j z_j^2 - \left|z_j\right|^{2q} - \frac{\sigma_j(1-q)}{2}\tilde{\lambda}_j^2 - \frac{\sigma_j}{2}\tilde{\lambda}_j^{2q}\right] \\ & + \sum_{j=1}^{n-1}\left[\frac{1}{4}\delta_j^2 + \frac{1}{2}a_j^2 + \frac{\sigma_j}{2}\lambda_j^2 + \frac{j}{4} + \frac{\sigma_j(1-q)}{2}\right] + y_n^2 \\ & + \sum_{j=2}^{n-1}\left[-\frac{1}{\tau_j}y_j^{2q} - \left(\frac{1}{\tau_j} - 2\right)y_j^2 + \frac{1}{4}\eta_j^2\right] + z_n\left[\theta_n^{*T}\phi_n(Z_n) + \varepsilon_n\right. \\ & \left. + u - |z_n|^{2q-1}\right] + \tilde{\lambda}_n\dot{\hat{\lambda}}_n + y_n\dot{y}_n + \frac{1}{4} + \frac{3}{2}z_n^2 + \frac{1}{2}d^2.\end{aligned} \tag{4.48}$$

Using Young's inequality yields

$$z_n\theta_n^{*T}\phi_n(Z_n) \leq \frac{\|\phi_n(Z_n)\|^2 z_n^2\lambda_n}{2a_n^2} + \frac{a_n^2}{2}, \tag{4.49}$$

where $a_n > 0$ is a design constant.

Therefore, Eq (4.48) can be transformed into the following form:

$$\begin{aligned}\dot{V}_n \leq & \sum_{j=1}^{n-1}\left[-k_j z_j^2 - \left|z_j\right|^{2q} - \frac{\sigma_j(1-q)}{2}\tilde{\lambda}_j^2 - \frac{\sigma_j}{2}\tilde{\lambda}_j^{2q}\right] \\ & + \sum_{j=1}^{n-1}\left[\frac{1}{4}\delta_j^2 + \frac{1}{2}a_j^2 + \frac{\sigma_j}{2}\lambda_j^2 + \frac{j}{4} + \frac{\sigma_j(1-q)}{2}\right] \\ & + \sum_{j=2}^{n-1}\left[-\frac{1}{\tau_j}y_j^{2q} - \left(\frac{1}{\tau_j} - 2\right)y_j^2 + \frac{1}{4}\eta_j^2\right] + \frac{3}{2}z_n^2 + y_n^2 \\ & + z_n\left[\frac{\|\phi_n(Z_n)\|^2 z_n\lambda_n}{2a_n^2} + u - |z_n|^{2q-1}\right] \\ & + \tilde{\lambda}_n\dot{\hat{\lambda}}_n + y_n\dot{y}_n + \frac{1}{4} + \frac{1}{2}d^2 + \frac{a_n^2}{2} + z_n\varepsilon_n.\end{aligned} \tag{4.50}$$

Construct the control signal u as follows:

$$u = -\left(k_n + \frac{5}{2}\right)z_n - \frac{\|\phi_n(Z_n)\|^2 z_n\hat{\lambda}_n}{2a_n^2}. \tag{4.51}$$

The updating law of $\hat{\lambda}_n$ is designed as follows:

$$\dot{\hat{\lambda}}_n = \frac{\|\phi_n(Z_n)\|^2 z_n^2}{2a_n^2} - \sigma_n\hat{\lambda}_n, \tag{4.52}$$

where k_n, σ_n are positive design constants. Substituting Eqs (4.51) and (4.52) into Eq (4.50), we have

$$\begin{aligned}\dot{V}_n \leq & \sum_{j=1}^{n}\left[-k_j z_j^2 - \left|z_j\right|^{2q} - \frac{\sigma_j(1-q)}{2}\tilde{\lambda}_j^2 - \frac{\sigma_j}{2}\tilde{\lambda}_j^{2q}\right] \\ & + \sum_{j=1}^{n}\left[\frac{1}{2}a_j^2 + \frac{\sigma_j}{2}\lambda_j^2 + \frac{j}{4} + \frac{\sigma_j(1-q)}{2}\right] \\ & + \sum_{j=2}^{n-1}\left[-\frac{1}{\tau_j}y_j^{2q} - \left(\frac{1}{\tau_j} - 2\right)y_j^2 + \frac{1}{4}\eta_j^2\right] + y_n^2 \\ & + y_n\dot{y}_n - z_n^2 + \frac{1}{2}d^2 + z_n\varepsilon_n + \sum_{j=1}^{n-1}\frac{1}{4}\delta_j^2.\end{aligned} \tag{4.53}$$

The non-negative continuous function $\delta_n\left(\bar{z}_n, \bar{y}_n, \overline{\tilde{\lambda}}_n, y_d, \dot{y}_d, r\right)$ satisfies

$$\left|\varepsilon_n\left(Z_n\right)\right| \leq \delta_n\left(\bar{z}_n, \bar{y}_n, \overline{\tilde{\lambda}}_n, y_d, \dot{y}_d, r\right).$$

Using Young's inequality yields

$$z_n\varepsilon_n \leq z_n^2 + \frac{1}{4}\delta_n^2. \tag{4.54}$$

Therefore, we have

$$\begin{aligned}\dot{V}_n \leq & \sum_{j=1}^{n}\left[-k_j z_j^2 - \left|z_j\right|^{2q} - \frac{\sigma_j(1-q)}{2}\tilde{\lambda}_j^2 - \frac{\sigma_j}{2}\tilde{\lambda}_j^{2q}\right] \\ & + \sum_{j=1}^{n}\left[\frac{1}{4}\delta_j^2 + \frac{1}{2}a_j^2 + \frac{\sigma_j}{2}\lambda_j^2 + \frac{j}{4} + \frac{\sigma_j(1-q)}{2}\right] \\ & + \sum_{j=2}^{n-1}\left[-\frac{1}{\tau_j}y_j^{2q} - \left(\frac{1}{\tau_j} - 2\right)y_j^2 + \frac{1}{4}\eta_j^2\right] + y_n^2 + y_n\dot{y}_n + \frac{1}{2}d^2.\end{aligned} \tag{4.55}$$

The nonlinear filter is designed as follows:

$$\dot{\omega}_n = -\frac{1}{\tau_n}\left|y_n\right|^{2q-1}\operatorname{sgn}\left(y_n\right) - \frac{1}{\tau_n}\left|y_n\right|\operatorname{sgn}\left(y_n\right), \tag{4.56}$$

where $y_n = \omega_n - \hbar_{n-1}$, and τ_n is a positive design constant.

The non-negative continuous function $\eta_n\left(\bar{s}_n, \bar{z}_n\bar{y}_n, \overline{\tilde{\lambda}}_n, y_d, \dot{y}_d, \ddot{y}_d, r, k_c(t), \dot{k}_c(t), \ddot{k}_c(t), \varpi, \dot{\varpi}, \ddot{\varpi}\right)$ satisfies

$$\left|-\dot{\hbar}_{n-1}\right| \leq \eta_n\left(\bar{s}_n, \bar{z}_n, \bar{y}_n, \overline{\tilde{\lambda}}_n, y_d, \dot{y}_d, \ddot{y}_d, r, k_c(t), \dot{k}_c(t), \ddot{k}_c(t), \varpi, \dot{\varpi}, \ddot{\varpi}\right) \tag{4.57}$$

From Eqs (4.56) and (4.57), we obtain

$$y_n\dot{y}_n = y_n\left(\dot{\omega}_n - \dot{\hbar}_{n-1}\right) = -\frac{1}{\tau_n}|y|_n^{2q} - \frac{1}{\tau_n}y_n^2 - y_n\dot{\hbar}_{n-1} \leq -\frac{1}{\tau_n}|y|_n^{2q} - \frac{1}{\tau_n}y_n^2 + y_n^2 + \frac{1}{4}\eta_n^2. \tag{4.58}$$

Therefore, we have

$$\begin{aligned}\dot{V}_n \le & \sum_{j=1}^{n}\left[-k_j z_j^2 - \left|z_j\right|^{2q} - \frac{\sigma_j(1-q)}{2}\tilde{\lambda}_j^2 - \frac{\sigma_j}{2}\tilde{\lambda}_j^{2q}\right] \\ & + \sum_{j=1}^{n}\left[\frac{1}{4}\delta_j^2 + \frac{1}{2}a_j^2 + \frac{\sigma_j}{2}\lambda_j^2 + \frac{j}{4} + \frac{\sigma_j(1-q)}{2}\right] \\ & + \sum_{j=2}^{n}\left[-\frac{1}{\tau_j}y_j^{2q} - \left(\frac{1}{\tau_j} - 2\right)y_j^2 + \frac{1}{4}\eta_j^2\right] + \frac{1}{2}d^2.\end{aligned} \tag{4.59}$$

5. Main results

Define the whole Lyapunov function V_n and two compact sets Ω, Ω_{k_c} as follows:

$$V_n = \sum_{j=1}^{n}\frac{1}{2}z_j^2 + \sum_{j=1}^{n}\frac{1}{2}\tilde{\lambda}_j^2 + \sum_{j=2}^{n}\frac{1}{2}y_j^2, \tag{5.1}$$

$$\Omega = \left\{\left[\bar{z}_n^T, \bar{y}_n^T, \bar{\tilde{\lambda}}_n^T, r\right]^T : \quad V_n \le P\right\}, \tag{5.2}$$

$$\Omega_{k_c} = \left\{\left[k_c, \dot{k}_c, \ddot{k}_c\right]^T : k_c^2 + \dot{k}_c^2 + \ddot{k}_c^2 \le P_{k_c}\right\}, \tag{5.3}$$

where P and $P_{k_c} > 0$. The maximum values of the continuous functions $\eta_i(\cdot)$ and $\delta_i(\cdot)$ on the compact set $\Omega \times \Omega_{k_c}$ are M_i and N_i, respectively.

Theorem 1. *Consider the closed-loop system which consists of the plant (1) under Assumptions 1 and 2, the control law given by Eq (4.51), virtual control laws given by Eqs (4.13) and (4.33), and adaptive laws given by Eqs (4.14), (4.34) and (4.52). If $V_n^q(0) \le P$ is true, then there exist some design constants σ_i, τ_i and k_i such that all signals in the closed-loop system are bounded, and the tracking error can converge to a preset region in finite-time, and the design constants σ_i, τ_i and k_i satisfy the following inequalities:*

$$\begin{cases} k_i > 0, \sigma_i > 0, \quad 1 \le i \le n, \\ \frac{1}{\tau_i} > 2, 2 \le i \le n, \\ \alpha = 2\min\left\{k_1, \ldots, k_n, \frac{1}{\tau_2} - 2, \ldots, \frac{1}{\tau_n} - 2, \sigma_1(1-q), \ldots, \sigma_n(1-q)\right\}, \\ \beta = 2^q \min\left\{1, \frac{\sigma_1}{2}, \ldots, \frac{\sigma_n}{2}, \frac{1}{\tau_2}, \ldots, \frac{1}{\tau_n}\right\}. \end{cases} \tag{5.4}$$

Proof. If $V_n^q \le P$, then $z_1, \ldots, z_n, y_2, \ldots, y_n, \hat{\lambda}_1, \ldots, \hat{\lambda}_n$ are bounded. Because $y_i = \omega_i - \hbar_{i-1}$ and y_i values are bounded, we can get ω_i, and $\hbar_{i-1}$ which are bounded. According to $x_i = z_i + y_i + \hbar_{i-1}$, we can obtain that x_i is bounded. Furthermore, it is known that the control signal u is bounded.

The time derivative of V_n is given by

$$\begin{aligned}
\dot{V}_n &\leq \sum_{j=1}^{n}\left[-k_j z_j^2 - |z_j|^{2q} - \frac{\sigma_j(1-q)}{2}\tilde{\lambda}_j^2 - \frac{\sigma_j}{2}\tilde{\lambda}_j^{2q}\right] \\
&\quad + \sum_{j=1}^{n}\left[\frac{1}{4}\delta_j^2 + \frac{1}{2}a_j^2 + \frac{\sigma_j}{2}\lambda_j^2 + \frac{j}{4} + \frac{\sigma_j(1-q)}{2}\right] \\
&\quad + \sum_{j=2}^{n}\left[-\frac{1}{\tau_j}y_j^{2q} - \left(\frac{1}{\tau_j} - 2\right)y_j^2 + \frac{1}{4}\eta_j^2\right] + \frac{1}{2}d^2 \\
&\leq \sum_{j=1}^{n}\left[-k_j z_j^2 - |z_j|^{2q} - \frac{\sigma_j(1-q)}{2}\tilde{\lambda}_j^2 - \frac{\sigma_j}{2}\tilde{\lambda}_j^{2q}\right] \\
&\quad + \sum_{j=1}^{n}\left[\frac{1}{4}N_j^2 + \frac{1}{2}a_j^2 + \frac{\sigma_j}{2}\lambda_j^2 + \frac{j}{4} + \frac{\sigma_j(1-q)}{2}\right] \\
&\quad + \sum_{j=2}^{n}\left[-\frac{1}{\tau_j}y_j^{2q} - \left(\frac{1}{\tau_j} - 2\right)y_j^2 + \frac{1}{4}M_j^2\right] + \frac{1}{2}d^2 \\
&\leq \sum_{j=1}^{n}\left[-k_j z_j^2 - |z_j|^{2q} - \frac{\sigma_j(1-q)}{2}\tilde{\lambda}_j^2 - \frac{\sigma_j}{2}\tilde{\lambda}_j^{2q}\right] \\
&\quad + \sum_{j=2}^{n}\left[-\frac{1}{\tau_j}y_j^{2q} - \left(\frac{1}{\tau_j} - 2\right)y_j^2\right] + \bar{C},
\end{aligned} \tag{5.5}$$

where

$$\bar{C} = \sum_{j=1}^{n}\left(\frac{1}{4}N_j^2 + \frac{1}{2}a_j^2 + \frac{\sigma_j}{2}\lambda_j^2 + \frac{j}{4} + \frac{\sigma_j(1-q)}{2}\right) + \sum_{j=2}^{n}\frac{1}{4}M_j^2 + \frac{1}{2}d^2.$$

Accordingly, the above equations can be rewritten as follows:

$$\dot{V}_n \leq -\alpha V_n - \beta V_n^q + \bar{C}, \tag{5.6}$$

where

$$\alpha = 2\min\left\{k_1, \ldots, k_n, \frac{1}{\tau_2} - 2, \cdots, \frac{1}{\tau_n} - 2, \sigma_1(1-q), \ldots, \sigma_n(1-q)\right\},$$

$$\beta = 2^q \min\left\{1, \frac{\sigma_1}{2}, \ldots, \frac{\sigma_n^2}{2}, \frac{1}{\tau_2}, \ldots, \frac{1}{\tau_n}\right\}.$$

If $V_n^q \leq P, \beta \geq \frac{\bar{C}}{P}$ and $V_n(0) \leq P$, then $\dot{V}_n \leq 0$. It implies that $\frac{dV_n^q}{dt} = qV_n^{q-1}\dot{V}_n \leq 0$. It can be seen that $V_n^q(t) \leq P, \forall t > 0$. Therefore, Eq (5.6) holds. According to Eq (5.6) and Lemma 2, we have the settling time $T_r = \frac{1}{\alpha(1-q)}\ln\frac{\alpha V^{1-q}(0)+\nu\beta}{\nu\beta}$. It yields that the closed-loop system exhibits SGPFTS for $t \geq T_r$. □

6. Numerical examples

In this section, we present numerical simulations that were conducted by using MATLAB/SIMULINK. We utilize two numerical examples to provide further illustration of the efficacy of the proposed control approach.

Example 1. *The first uncertain nonlinear system is selected as follows:*

$$\begin{cases} \dot{\hbar} = -\hbar + 0.5x_1^2 \sin(x_1 t), \\ \dot{x}_1 = x_1 + x_2 + \frac{x_2^3}{5} + d_1, \\ \dot{x}_2 = x_3 + \frac{x_3^3}{2} + d_2, \\ \dot{x}_3 = x_1 x_2 x_3 + q(u) + d_3, \\ y = x_1, \end{cases} \tag{6.1}$$

where $d_1 = 2\hbar\sin(t), d_2 = 0.1\hbar\cos(x_1 x_3 t)$, *and* $d_3 = 0.2\hbar\cos(0.5x_2 t) - 0.5x_1$. *The desired tracking trajectory* $y_d(t) = 0.5[\sin(t) + \sin(0.5t)]$. *The dynamic signal is set as* $\dot{r} = -r + 2.5x_1^4 + 0.625$.

The adaptive control algorithm is set as follows:

$$u = -\left(k_3 + \frac{5}{2}\right) z_3 - \frac{\|\phi_3(Z_3)\|^2 z_3 \hat{\lambda}_3}{2a_3^2}, \tag{6.2}$$

$$\hbar_1 = -\frac{1}{m}\left[\left(k_1 + 1 + \frac{1}{2}m^2\right) z_1 + \frac{\|\phi_1(Z_1)\|^2 z_1 \hat{\lambda}_1}{2a_1^2}\right], \tag{6.3}$$

$$\hbar_2 = -\left(k_2 + \frac{5}{2}\right) z_2 - \frac{\|\phi_2(Z_2)\|^2 z_2 \hat{\lambda}_2}{2a_2^2}, \tag{6.4}$$

$$\dot{\hat{\lambda}}_1 = \frac{\|\phi_1(Z_1)\|^2 z_1^2}{2a_1^2} - \sigma_1 \hat{\lambda}_1, \tag{6.5}$$

$$\dot{\hat{\lambda}}_2 = \frac{\|\phi_2(Z_2)\|^2 z_2^2}{2a_2^2} - \sigma_2 \hat{\lambda}_2, \tag{6.6}$$

$$\dot{\hat{\lambda}}_3 = \frac{\|\phi_3(Z_3)\|^2 z_3^2}{2a_3^2} - \sigma_3 \hat{\lambda}_3, \tag{6.7}$$

$$\dot{\omega}_2 = -\frac{1}{\tau_2}|y_2|^{2q-1}\operatorname{sgn}(y_2) - \frac{1}{\tau_2}|y_2|\operatorname{sgn}(y_2), \tag{6.8}$$

$$\dot{\omega}_3 = -\frac{1}{\tau_3}|y_3|^{2q-1}\operatorname{sgn}(y_3) - \frac{1}{\tau_3}|y_3|\operatorname{sgn}(y_3), \tag{6.9}$$

where

$$z_1 = S = \frac{1}{2}\log\frac{k_c(t) + \frac{e_1}{\varpi}}{k_c(t) - \frac{e_1}{\varpi}},$$

$$z_2 = s_2 - \omega_2,$$

$$z_3 = s_3 - \omega_3,$$

$$Z_1 = \left[\bar{x}_2^T, z_1, y_d, \dot{y}_d, \varpi, \dot{\varpi}, k_c(t), \dot{k}_c(t), r\right]^T \in R^{10},$$

$$Z_2 = \left[\bar{x}_3^T, z_2, y_2, r\right]^T \in R^6,$$

$$Z_3 = \left[\bar{x}_3^T, z_3, y_3, r\right]^T \in R^6,$$

$$y_2 = \omega_2 - \hbar_1,$$

$$y_3 = \omega_3 - \hbar_2.$$

Choosing the PPF as $\varpi(t) = 0.7e^{-3t} + 0.1$, *the time-varying constraint function as* $k_c(t) = 0.7 + 0.2\cos t$, *and* $m(t) = \frac{1}{k_c(t)\varpi\left(1-\tanh^2 S\right)}$, *the dynamic signal is set as* $\dot{r} = -r + 1.5x_1^4 + 0.8$. *Initial values are set as* $x_1(0) = 0.2, x_2(0) = 0.1, x_3(0) = 0.15, \hat{\lambda}_1(0) = 0.1, \hat{\lambda}_2(0) = 0.6, \hat{\lambda}_3(0) = 0.3, \omega_2(0) = 0.1, \omega_3(0) = 0.2, r(0) = 0.3, \hbar(0) = 0.1$, *and* $l_1 = l_2 = 10$. *The design constants are selected as* $k_1 = 2, k_2 = 50, a_1 = a_2 = 1, \sigma_1 = 0.1, \sigma_2 = 0.1, \tau_2 = 0.3, q = 0.5, p = \frac{3}{17}, u_{\min} = 0.2, u_{th} = \frac{u_{10}}{1-\delta}, \delta = \frac{1-p}{1+p}$, *and* $u_{\min} = p^{1-i}u_{\min}, i = 1, 2, \ldots, \infty$.

As depicted in Figures 1, it is evident that the output signal adeptly tracks the desired trajectory, with the tracking error converging to a predetermined region. Figure 2 illustrates the disparity between the quantization signal $q(u)$ and the control signal u. The small quantization error and the effective discretization of the continuous signal are evident from Figure 3. Furthermore, Figure 4 demonstrates that the updating parameters $\hat{\lambda}_1, \hat{\lambda}_2, \hat{\lambda}_3$ remain bounded. These observations collectively affirm the robust performance and stability of the proposed control methodology.

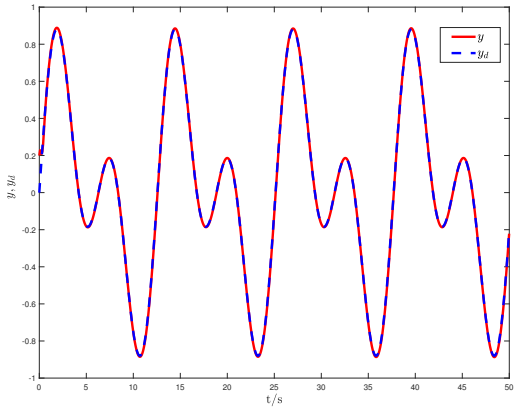

Figure 1. Output y (solid line) and desired trajectory y_d (dashed line).

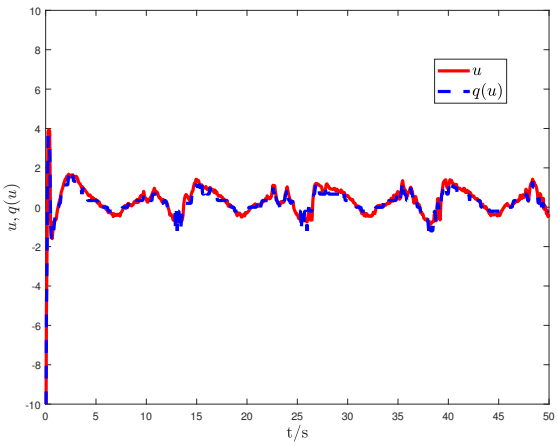

Figure 2. Quantization signal $q(u)$ (solid line) and control signal u (dashed line).

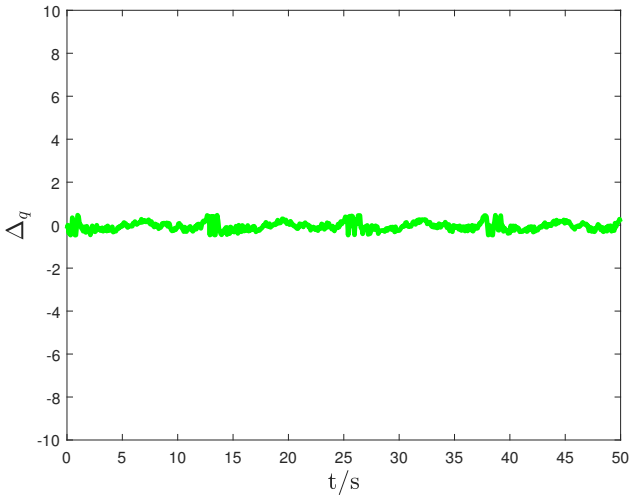

Figure 3. Quantization error Δ_q.

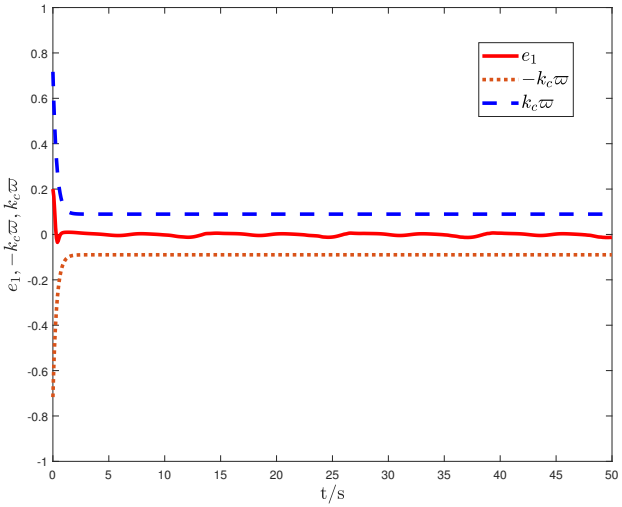

Figure 4. Prescribed performance $-k_c\varpi$ (dotted-dashed line), $k_c\varpi$ (dashed line) and tracking error e_1 (solid line).

Example 2. *Consider a ship's dynamic system; its dynamic equation is described as follows:*

$$\ddot{v} + J\dot{v} + l\left(Mv^3 + Bv\right) = lq(u) \tag{6.10}$$

where v stands for the angular velocity of the ship course, $q(u)$ is the input quantization, $l \neq 0$, M and B represent unknown constants of the ship related hydrodynamic coefficients and ship mass, respectively, and $J = 0.2$, where we set $l = 1.8, M = 0.12$, and $B = 0.2$. Define $x_1 = v, x_2 = \dot{b}$. The ship's dynamic system with unmodeled dynamics, input quantization and prescribed performance can be described as follows:

$$\begin{cases} \dot{\hbar} = -\hbar + 0.5x_1^2 \sin(x_1 t), \\ \dot{x}_1 = x_2 + 2\hbar \sin(t), \\ \dot{x}_2 = -0.2x_2 - 1.8\left(0.12x_1^3 + 0.2x_1\right) + 1.8q(u) + 0.2\hbar \cos(0.5x_2 t) - 0.5x_1, \\ y = x_1. \end{cases} \tag{6.11}$$

Choosing the initial values as $x_1(0) = 0.3, x_2(0) = 0.2, \hat{\lambda}_1(0) = 2, \hat{\lambda}_2(0) = 0.5, \omega_2(0) = 0.1, r(0) = 0.1$, *and* $\hbar(0) = 0.1$, *and setting the design constants to* $a_1 = a_2 = 1, \sigma_1 = 0.1, \sigma_2 = 0.1, \tau_2 = 0.3, k_1 = 2, k_2 = 100, q = 0.6, p = \frac{3}{17}, u_{\min} = 0.2$, *and* $l_1 = l_2 = 10$, *we chose the desired signal as* $y_d = 1.5\sin(0.6t)$ *and the auxiliary signal as* $\dot{r} = -r + 1.5x_1^4 + 0.8$. *The simulation results are shown in Figures 5–8. It can be ascertained from Figure 5 that this method has good performance in terms of the prescribed tracking. Figure 6 shows the difference between the quantization signal* $q(u)$ *and the control signal* u, *and the quantization error is small. Figures 7 and 8 show that the control signal* u *and adaptive tuning parameters* $\hat{\lambda}_1, \hat{\lambda}_2$ *are bounded.*

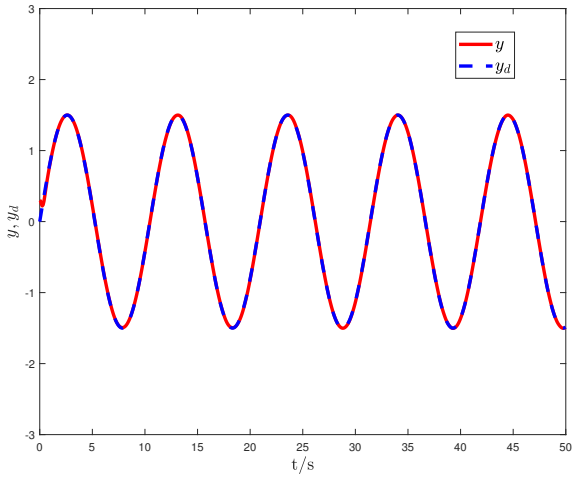

Figure 5. Output y (solid line) and desired trajectory y_d (dashed line).

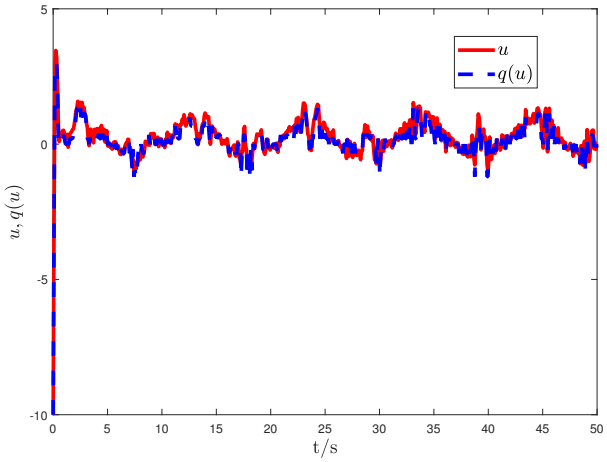

Figure 6. Quantization signal $q(u)$ (solid line) and control signal u (dashed line).

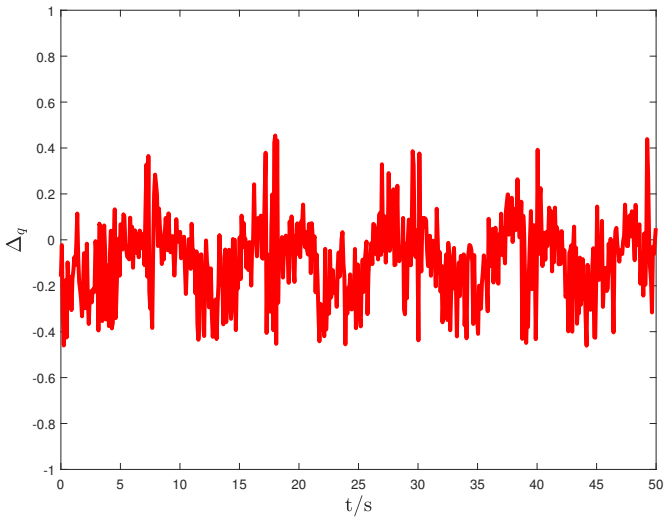

Figure 7. Quantization error Δ_q.

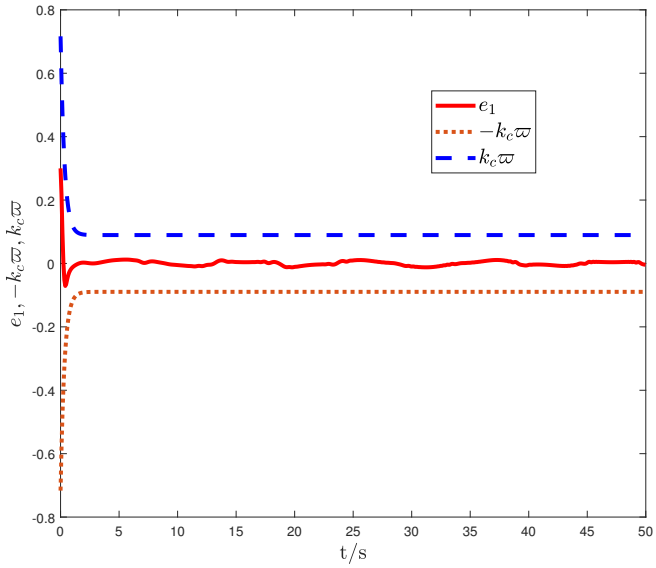

Figure 8. Prescribed performance $-k_c\varpi$ (dotted-dashed line), $k_c\varpi$ (dashed line) and tracking error e_1 (solid line).

Example 3. *To validate the effectiveness of the proposed control scheme in this paper, simulations and comparisons of different control methods were conducted on the same pure-feedback system with input quantization and unmodeled dynamics. The proposed finite-time DSC (referred to as FTDSC) in this paper is compared to the traditional DSC.*

A pure-feedback system with input quantization and unmodeled dynamics was evaluated:

$$\begin{cases} \dot{\xi} = -\xi + 0.5x_1^2 \sin(x_1 t), \\ \dot{x}_1 = x_1 + x_2 + \frac{x_2^3}{5} + 2\xi \sin(t), \\ \dot{x}_2 = x_1 x_2 + q(u) + 0.2\xi \cos(0.5x_2 t) - 0.5x_1, \\ y = x_1. \end{cases} \tag{6.12}$$

In the proposed FTDSC method in this paper, the virtual control law is chosen as

$$\hbar_1 = -\frac{1}{m}\left(\left(k_1 + 1 + \frac{1}{2}m^2\right)z_1 + \frac{\|\phi_1(Z_1)\|^2 z_1 \hat{\lambda}_1}{2a_1^2}\right). \tag{6.13}$$

Then, the control law u_{FTDSC} is applied as follows

$$u_{FTDSC} = -\left(k_2 + \frac{5}{2}\right)z_2 - \frac{\|\phi_2(Z_2)\|^2 z_2 \hat{\lambda}_2}{2a_2^2}. \tag{6.14}$$

We selected the parameters as $k_1 = 2, k_2 = 50, a_1 = a_2 = 1, \sigma_1 = 0.1, \sigma_2 = 0.1, \tau_2 = 0.3, q = 0.5, p = \frac{3}{17}, u_{\min} = 0.2, u_{th} = \frac{u_{10}}{1-\delta}$, $l = 5$, and $\delta = \frac{1-p}{1+p}$.

To ensure a fair comparison in the simulation, based on the pure feedback system described by Eq (6.12), the virtual control law has been designed as follows

$$\alpha_1 = -\frac{c_1 z_1}{\mu_1} - \frac{z_1 \hat{\lambda}\|\Psi(X)\|}{2a_0^2 \mu_1}. \tag{6.15}$$

Then, the control law u_{DSC} is designed was follows

$$u = -u_2 \tanh\left(\frac{z_2 u_2}{r}\right), \tag{6.16}$$

where $u_2 = -\frac{\alpha_2}{1-\delta}$, $\alpha_2 = -c_2 z_2 - k_2 l^2 (y - \hat{x}_1) + \dot{\omega}_2 - z_2$.

Similarly, the parameters selected based on the traditional DSC control method were as follows: $k_1 = 2, k_2 = 2, c_1 = 40, c_2 = 10, \sigma = 0.01, \tau_2 = 0.01$, $l = 5, a_0 = 5, p = \frac{3}{17}, u_{\min} = 0.2, \delta = \frac{1-p}{1+p}$, and $r = 0.2$.

We selected the desired signal as $y_d = 0.5(\sin(t) + \sin(0.5t))$ and the dynamic signal as $\dot{r} = -r + 1.5y^4 + 0.8$, with the initial values set as $x_1(0) = 0.1, x_2(0) = 0.1, r(0) = 0.1, \hat{\lambda}(0) = 0.1, \omega_2(0) = 0.1$, and $\xi(0) = 0.1$. The comparative simulation results are shown in Figures 9–12.

In Figure 9a, the red solid line represents the desired tracking trajectory y_d, the blue dashed line represents the output signal y in the proposed FTDSC, and the green dashed line represents the output signal in the traditional DSC method. Figure 9b is a partial enlarged view of Figure 9a. From the local zoom-in, it can be observed that under both control methods, the output signal y can effectively track the desired trajectory y_d. However, from the local zoom-in plot in (b), it is evident that the tracking performance of the FTDSC method is superior to the traditional DSC method, with a faster convergence speed. In Figure 10, the red solid line represents the tracking error $y - y_d$ in the FTDSC method, while the black dashed line represents the tracking error $y - y_d$ in the DSC method. It can be observed from the local magnification that the tracking error in the FTDSC method is smaller. In Figure 11, in subfigures (a) and (b), the red dashed line represents the quantized signal $q(u)$, and the blue dashed line represents the control signal u. In Figure 12, the blue dashed line represents the

quantization error $q(u) - u$ in the FTDSC method, and the red dashed line represents the quantization error $q(u) - u$ in the traditional DSC method. Combining the local magnification chart in Figure 12, it can be observed that the FTDSC method has smaller quantization errors than the DSC method, indicating greater accuracy.

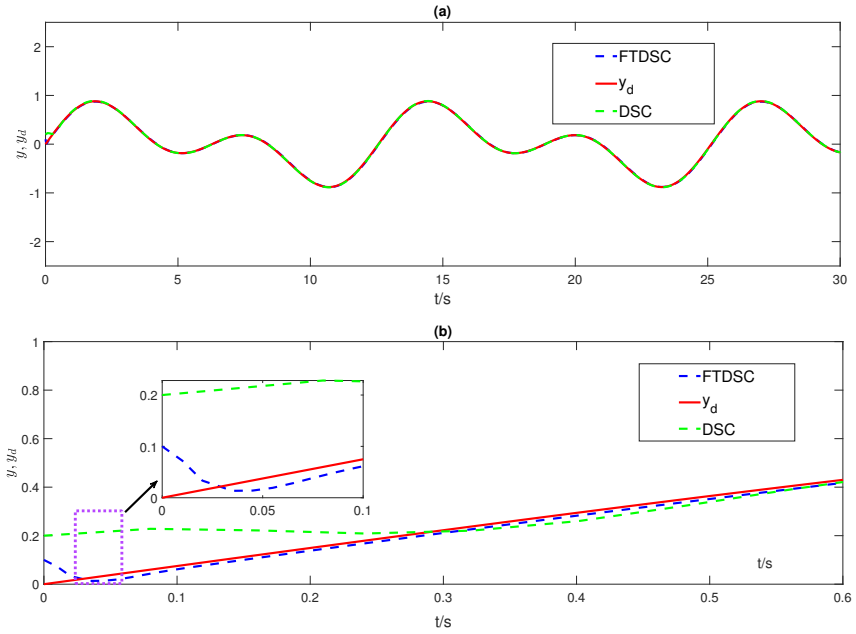

Figure 9. The output y and its tracking under two methods.

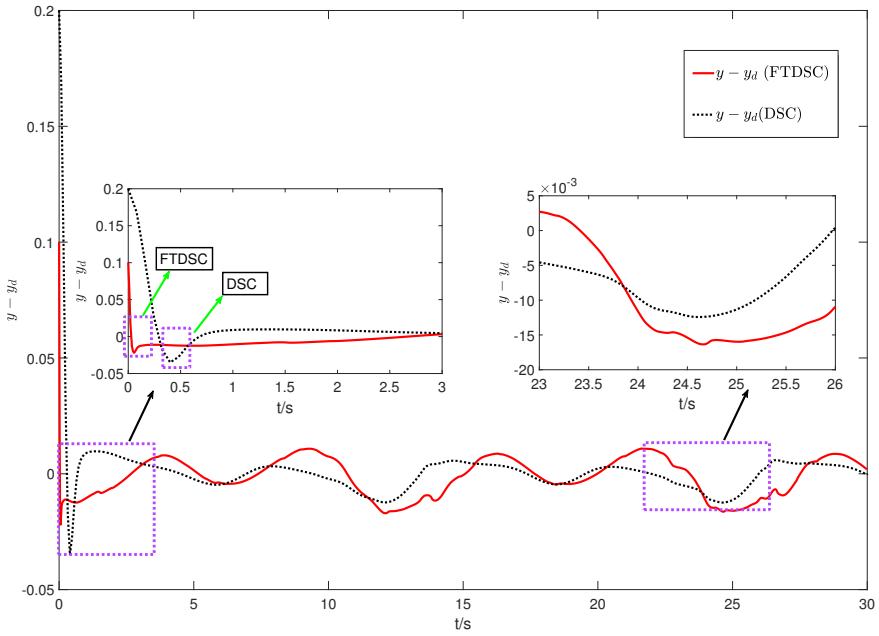

Figure 10. Tracking error of output y under two methods.

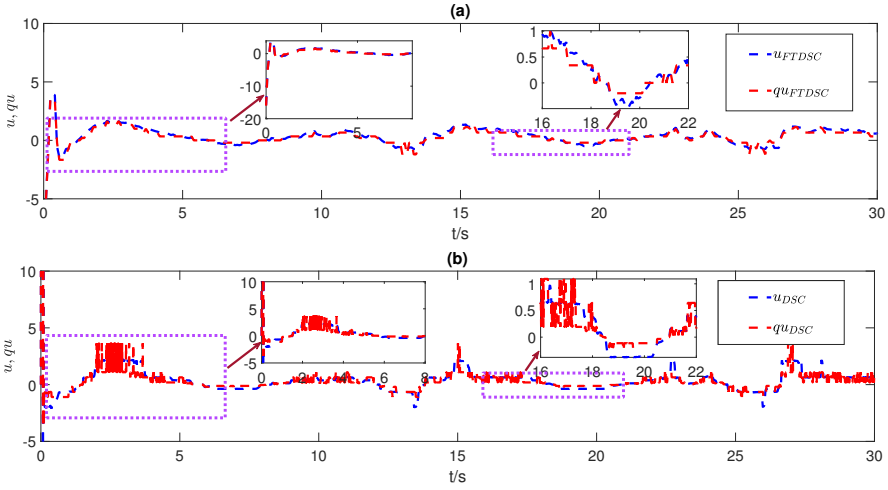

Figure 11. The control signals u and quantized control signals $q(u)$ under two control methods.

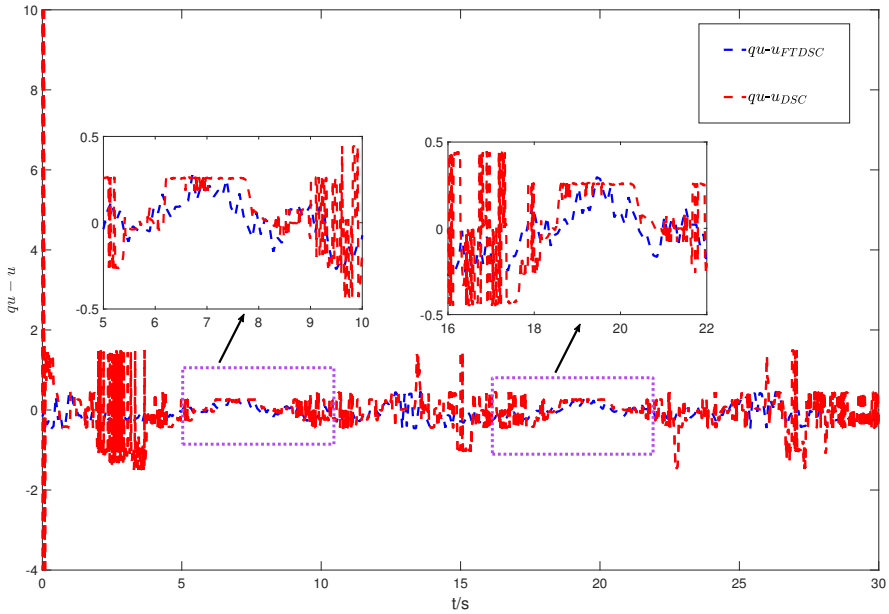

Figure 12. The quantization error under two methods.

7. Conclusions

In this paper, a new finite-time adaptive control scheme has been presented for non-affine nonlinear systems subject to input quantization, unmodeled dynamics and prescribed performance. An invertible nonlinear mapping has been formulated by leveraging the characteristics of the hyperbolic tangent function. The development of a novel controller has been achieved through the incorporation of a

nonlinear filter and the application of Young's inequality, coupled with an improved DSC strategy. The issue of "complexity explosion" that is inherent in traditional backstepping is successfully mitigated, while the problem of "singularity" in finite time is eliminated. Compared with the previous first-order linear filter, the nonlinear filter reduces the demand on the time constant. Theoretical analysis indicates that all signals within the controlled process are bounded within finite time, and that the tracking error of the system can converge to a predefined time-varying region within a finite duration. Simulation curves substantiate the effectiveness of the proposed design scheme.

Our future work will be aimed at exploring the potential integration of machine learning technologies, such as reinforcement learning or neural networks, to solve complex system dynamics and uncertainties. In addition, it will be an important aspect of our future research work to study the scalability and robustness of the controller under large-scale systems and different operating conditions.

Use of AI tools declaration

The authors declare they have not used Artificial Intelligence (AI) tools in the creation of this article.

Acknowledgments

This work was partially supported by the Jiangsu University "Blue Project" Outstanding Young Key Teachers Fund.

Conflict of interest

The authors declare that there are no conflicts of interest.

References

1. I. Kanellakopoulos, P. V. Kokotovic, A. S. Morse, Systematic design of adaptive controllers for feedback linearizable systems, *1991 American Control Conference*, 1991, 649–654. https://doi.org/10.23919/ACC.1991.4791451
2. D. Swaroop, J. Karl Hedrick, P. P. Yip, J. Christian Gerdes, Dynamic surface control for a class of nonlinear systems, *IEEE Trans. Automat. Contr.*, **45** (2000), 1893–1899. https://doi.org/10.1109/TAC.2000.880994
3. H. Liu, T. Zhang, X. Xia, Adaptive neural dynamic surface control of MIMO pure-feedback nonlinear systems with output constraints, *Neurocomputing*, **333** (2019), 101–109. https://doi.org/10.1016/j.neucom.2018.12.011
4. M. Chiang, L. Fu, Adaptive stabilization of a class of uncertain switched nonlinear systems with backstepping control, *Automatica*, **50** (2014), 2128–2135. https://doi.org/10.1016/j.automatica.2014.05.029
5. T. Zhang, H. Xu, Adaptive optimal dynamic surface control of strict-feedback nonlinear systems with output constraints, *Int. J. Robust Nonlinear Control*, **30** (2020), 2059–2078. https://doi.org/10.1002/rnc.4864

6. B. Niu, X. Liu, Z. Guo, H. Jiang, H. Wang, Adaptive intelligent control-based consensus tracking for a class of switched non-strict feedback nonlinear multi-agent systems with unmodeled dynamics, *IEEE Trans. Artif. Intell.*, 2023, 1–11. https://doi.org/10.1109/TAI.2023.3300818
7. L. Zhao, J. Li, H. Li, B. Liu, Double-loop tracking control for a wheeled mobile robot with unmodeled dynamics along right angle roads, *ISA Trans.*, **136** (2023), 525–534. https://doi.org/10.1016/j.isatra.2022.10.045
8. J. Zhai, H. Wang, J. Tao, Z. He, Observer-based adaptive fuzzy finite time control for non-strict feedback nonlinear systems with unmodeled dynamics and input delay, *Nonlinear Dyn.*, **111** (2023), 1417–1440. https://doi.org/10.1007/s11071-022-07913-6
9. Z. Jiang, L. Praly, Design of robust adaptive controllers for nonlinear systems with dynamic uncertainties, *Automatica*, **34** (1998), 825–840. https://doi.org/10.1016/S0005-1098(98)00018-1
10. Y. Hua, T. Zhang, Adaptive control of pure-feedback nonlinear systems with full-state time-varying constraints and unmodeled dynamics, *Int. J. Adapt. Control Signal Process.*, **34** (2020), 183–198. https://doi.org/10.1002/acs.3077
11. T. P. Zhang, N. N. Wang, M. Z. Xia, Adaptive output feedback control of systems with unmodeled dynamics and output constraint, *Control Decis.*, **32** (2017), 55–62.
12. T. Zhang, M. Xia, J. Zhu, Adaptive backstepping neural control of state-delayed nonlinear systems with full-state constraints and unmodeled dynamics, *Int. J. Adapt. Control Signal Process.*, **31** (2017), 1704–1722. https://doi.org/10.1002/acs.2795
13. Y. Hua, T. Zhang, Adaptive neural event-triggered control of MIMO pure-feedback systems with asymmetric output constraints and unmodeled dynamics, *IEEE Access*, **8** (2020), 37684–37696. https://doi.org/10.1109/ACCESS.2020.2975618
14. X. Zhang, Y. Lin, Adaptive tracking control for a class of pure-feedback non-linear systems including actuator hysteresis and dynamic uncertainties, *IET Control Theory Appl.*, **5** (2011), 1868–1880. https://doi.org/10.1049/iet-cta.2010.0711
15. P. Li, N. Shlezinger, H. Zhang, B. Wang, Y. C. Eldar, Graph signal compression by joint quantization and sampling, *IEEE Trans. Signal Process.*, **70** (2022), 4512–4527. https://doi.org/10.1109/TSP.2022.3205474
16. Z. Ning, T. Wang, K. Zhang, Dynamic event-triggered security control and fault detection for nonlinear systems with quantization and deception attack, *Inf. Sci.*, **594** (2022), 43–59. https://doi.org/10.1016/j.ins.2022.02.019
17. C. De Persis, F. Mazenc, Stability of quantized time-delay nonlinear systems: a Lyapunov-Krasowskii-functional approach, *Math. Control Signals Syst.*, **21** (2010), 337–370. https://doi.org/10.1007/s00498-010-0048-1
18. T. Liu, Z. Jiang, D. J. Hill, A sector bound approach to feedback control of nonlinear systems with state quantization, *Automatica*, **48** (2012), 145–152. https://doi.org/10.1016/j.automatica.2011.09.041
19. L. Xing, C. Wen, Y. Zhu, H. Su, Z. Liu, Output feedback control for uncertain nonlinear systems with input quantization, *Automatica*, **65** (2016), 191–202. https://doi.org/10.1016/j.automatica.2015.11.028

20. X. Xia, T. Zhang, Robust adaptive quantized DSC of uncertain pure-feedback nonlinear systems with time-varying output and state constraints, *Int. J. Robust Nonlinear Control*, **28** (2018), 3357–3375. https://doi.org/10.1002/rnc.4087
21. M. Wang, T. Zhang, Y. Yang, Adaptive neural output feedback control for uncertain nonlinear systems with input quantization and output constraints, *Int. J. Adapt. Control Signal Process.*, **34** (2020), 228–247. https://doi.org/10.1002/acs.3079
22. W. Liu, D. W. C. Ho, S. Xu, B. Zhang, Adaptive finite-time stabilization of a class of quantized nonlinearly parameterized systems, *Int. J. Robust Nonlinear Control*, **27** (2017), 4554–4573. https://doi.org/10.1002/rnc.3813
23. F. Wang, B. Chen, C. Lin, J. Zhang, X. Meng, Adaptive neural network finite-time output feedback control of quantized nonlinear systems, *IEEE Trans. Cybernetics*, **48** (2017), 1839–1848. https://doi.org/10.1109/TCYB.2017.2715980
24. D. Huang, T. Huang, N. Qin, Y. Li, Y. Yang, Finite-time control for a UAV system based on finite-time disturbance observer, *Aerosp. Sci. Technol.*, **129** (2022), 107825. https://doi.org/10.1016/j.ast.2022.107825
25. Y. Li, B. Niu, G. Zong, J. Zhao, X. Zhao, Command filter-based adaptive neural finite-time control for stochastic nonlinear systems with time-varying full-state constraints and asymmetric input saturation, *Int. J. Syst. Sci.*, **53** (2022), 199–221. https://doi.org/10.1080/00207721.2021.1943562
26. S. P. Bhat, D. S. Bernstein, Continuous finite-time stabilization of the translational and rotational double integrators, *IEEE Trans. Automat. Contr.*, **43** (1998), 678–682. https://doi.org/10.1109/9.668834
27. S. P. Bhat, D. S. Bernstein, Finite-time stability of continuous autonomous systems, *SIAM J. Control Optim.*, **38** (2000), 751–766. https://doi.org/10.1137/S0363012997321358
28. G. Chen, Y. Yang, Finite-time stability of switched nonlinear time-varying systems via indefinite Lyapunov functions, *Int. J. Robust Nonlinear Control*, **28** (2018), 1901–1912. https://doi.org/10.1002/rnc.3968
29. R. Yang, L. Sun, Finite-time robust control of a class of nonlinear time-delay systems via lyapunov functional method, *J. Franklin Inst.*, **356** (2019), 1155–1176. https://doi.org/10.1016/j.jfranklin.2018.08.029
30. Y. Liu, Y. W. Jing, X. P. Liu, X. H. Li, Survey on finite-time control for nonlinear systems, *Control Theory Appl.*, **37** (2020), 1–12.
31. H. Li, S. Zhao, W. He, R. Lu, Adaptive finite-time tracking control of full state constrained nonlinear systems with dead-zone, *Automatica*, **100** (2019), 99–107. https://doi.org/10.1016/j.automatica.2018.10.030
32. Y. Huang, J. Wang, F. Wang, B. He, Event-triggered adaptive finite-time tracking control for full state constraints nonlinear systems with parameter uncertainties and given transient performance, *ISA Trans.*, **108** (2021), 131–143. https://doi.org/10.1016/j.isatra.2020.08.022
33. X. Jin, Adaptive fixed-time control for MIMO nonlinear systems with asymmetric output constraints using universal barrier functions, *IEEE Trans. Automat. Contr.*, **64** (2018), 3046–3053. https://doi.org/10.1109/TAC.2018.2874877

34. J. Cai, C. Wen, L. Xing, Q. Yan, Decentralized backstepping control for interconnected systems with non-triangular structural uncertainties, *IEEE Trans. Automat. Contr.*, **68** (2022), 1692–1699. https://doi.org/10.1109/TAC.2022.3152083
35. F. Doostdar, H. Mojallali, An ADRC-based backstepping control design for a class of fractional-order systems, *ISA Trans.*, **121** (2022), 140–146. https://doi.org/10.1016/j.isatra.2021.03.033
36. X. Yu, X. Meng, X. Zheng, Y. Liu, Improved adaptive backstepping control of MPCVD reactor systems with non-parametric uncertainties, *J. Franklin Inst.*, **360** (2023), 2182–2192. https://doi.org/10.1016/j.jfranklin.2022.09.052
37. Y. Li, K. Li, S. Tong, Finite-time adaptive fuzzy output feedback dynamic surface control for MIMO nonstrict feedback systems, *IEEE Trans. Fuzzy Syst.*, **27** (2018), 96–110. https://doi.org/10.1109/TFUZZ.2018.2868898
38. J. Li, Y. Yang, C. Hua, X. Guan, Fixed-time backstepping control design for high-order strict-feedback non-linear systems via terminal sliding mode, *IET Control Theory Appl.*, **11** (2017), 1184–1193. https://doi.org/10.1049/iet-cta.2016.1143
39. L. Liu, T. Gao, Y. Liu, S. Tong, Time-varying asymmetrical BLFs based adaptive finite-time neural control of nonlinear systems with full state constraints, *IEEE/CAA J. Autom. Sin.*, **7** (2020), 1335–1343. https://doi.org/10.1109/JAS.2020.1003213
40. C. Liu, H. Wang, X. Liu, Y. Zhou, S. Lu, Adaptive prescribed performance tracking control for strict-feedback nonlinear systems with zero dynamics, *Int. J. Robust Nonlinear Control*, **29** (2019), 6507–6521. https://doi.org/10.1002/rnc.4739
41. W. Shi, Observer-based adaptive fuzzy prescribed performance control for feedback linearizable MIMO nonlinear systems with unknown control direction, *Neurocomputing*, **368** (2019), 99–113. https://doi.org/10.1016/j.neucom.2019.08.066
42. X. Xia, T. Zhang, Y. Yi, Q. Shen, Adaptive prescribed performance control of output feedback systems including input unmodeled dynamics, *Neurocomputing*, **190** (2016), 226–236. https://doi.org/10.1016/j.neucom.2016.01.014
43. J. Yu, P. Shi, L. Zhao, Finite-time command filtered backstepping control for a class of nonlinear systems, *Automatica*, **92** (2018), 173–180. https://doi.org/10.1016/j.automatica.2018.03.033

AIMS Press